JACS
JOURNAL OF THE AMERICAN CHEMICAL SOCIETY
Article
pubs.acs.org/JACS

Photoacidic and Photobasic Behavior of Transition Metal Compounds with Carboxylic Acid Group(s)

Ryan M. O'Donnell, Renato N. Sampaio, Guocan Li, Patrik G. Johansson, Cassandra L. Ward, and Gerald J. Meyer*

Department of Chemistry, University of North Carolina at Chapel Hill, Chapel Hill, North Carolina 27599, United States

Supporting Information

ABSTRACT: Excited state proton transfer studies of six Ru polypyridyl compounds with carboxylic acid/carboxylate group(s) revealed that some were photoacids and some were photobases. The compounds $[Ru^{II}(btfmb)_2(LL)]^{2+}$, $[Ru^{II}(dtb)_2(LL)]^{2+}$, and $[Ru^{II}(bpy)_2(LL)]^{2+}$, where bpy is 2,2′-bipyridine, btfmb is 4,4′-$(CF_3)_2$-bpy, and dtb is 4,4′-$((CH_3)_3C)_2$-bpy, and LL is either dcb = 4,4′-$(CO_2H)_2$-bpy or mcb = 4-(CO_2H),4′-(CO_2Et)-2,2′-bpy, were synthesized and characterized. The compounds exhibited intense metal-to-ligand charge-transfer (MLCT) absorption bands in the visible region and room temperature photoluminescence (PL) with long τ > 100 ns excited state lifetimes. The mcb compounds had very similar ground state pK_a's of 2.31 ± 0.07, and their characterization enabled accurate determination of the two pK_a values for the commonly utilized dcb ligand, pK_{a1} = 2.1 ± 0.1 and pK_{a2} = 3.0 ± 0.2. Compounds with the btfmb ligand were photoacidic, and the other compounds were photobasic. Transient absorption spectra indicated that btfmb compounds displayed a $[Ru^{III}(btfmb^-)L_2]^{2+*}$ localized excited state and a $[Ru^{III}(dcb^-)L_2]^{2+*}$ formulation for all the other excited states. Time dependent PL spectral shifts provided the first kinetic data for excited state proton transfer in a transition metal compound. PL titrations, thermochemical cycles, and kinetic analysis (for the mcb compounds) provided self-consistent pK_a* values. The ability to make a single ionizable group photobasic *or* photoacidic through ligand design was unprecedented and was understood based on the orientation of the lowest-lying MLCT excited state dipole relative to the ligand that contained the carboxylic acid group(s).

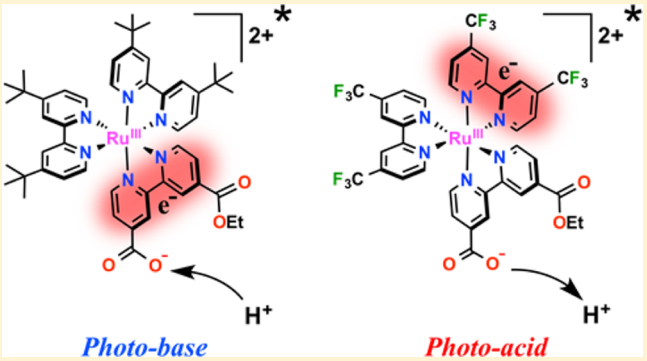

INTRODUCTION

Chromophores with Brønsted acidic or basic functional groups often exhibit excited-state acid−base behavior that differs significantly from that of the ground state.[1,2] Weber first observed such behavior back in 1931, and studies since have exploited this behavior for application as pH sensors,[3−5] photopolymerization,[6−8] synthesis,[9] solar-fuel production,[10] biological probes,[11−14] molecular switches,[15,16] as well as for fundamental studies of proton transfer and/or proton coupled electron transfer (PCET) reactions[17−19] as has been the subject of several reviews.[20−24] This chemistry is understood though the very familiar acid−base equilibrium which in this case is between a carboxylic acid $R(CO_2H)$, and its conjugate carboxylate $R(CO_2^-)$, defined by an equilibrium constant, K_a, eq 1. Light absorption by the acid form generates an excited state, HA*, that may release a proton to a greater extent than the ground state and hence is termed a *photoacid*, eq 2.

$$R(CO_2H) \overset{K_a}{\rightleftharpoons} R(CO_2^-) + H^+ \quad (1)$$

$$R(CO_2H)^* \overset{K_a^*}{\rightleftharpoons} R(CO_2^-)^* + H^+ \quad (2)$$

Likewise, light absorption by the conjugate base $R(CO_2^-)$ forms $R(CO_2^-)^*$ that may accept a proton and acts as a *photobase.* Under steady state illumination, a quasi-equilibrium defined by K_a* can be achieved wherein the solution concentrations remain invariant with time. The net change in acid−base chemistry with illumination is often quantified by the magnitude of $\Delta pK_a = pK_a^* - pK_a$.[1,22] It is quite usual to find that the acid dissociation constant of the protonated forms of the compounds change by 4−10 pK_a units upon light absorption. Here we report pK_a and pK_a* values, as well as the first excited state proton transfer rate constants, for a series of six Ru(II) polypyridyl compounds with one or two pendant carboxylic acid groups.

The increased basicity or acidity of an excited state reflects the redistribution of electron density that results from photon absorption and is of fundamental interest in its own right.[1,2] Reviews of excited-state acid−base chemistry teach that the identity of the ionizable functional group dictates whether light excitation will produce a photoacid or a photobase *without regard* to the nature of the excited state.[1,2,22,25] For example, phenols are

Received: January 20, 2016
Published: February 22, 2016

DOI: 10.1021/jacs.6b00454
J. Am. Chem. Soc. 2016, 138, 3891−3903

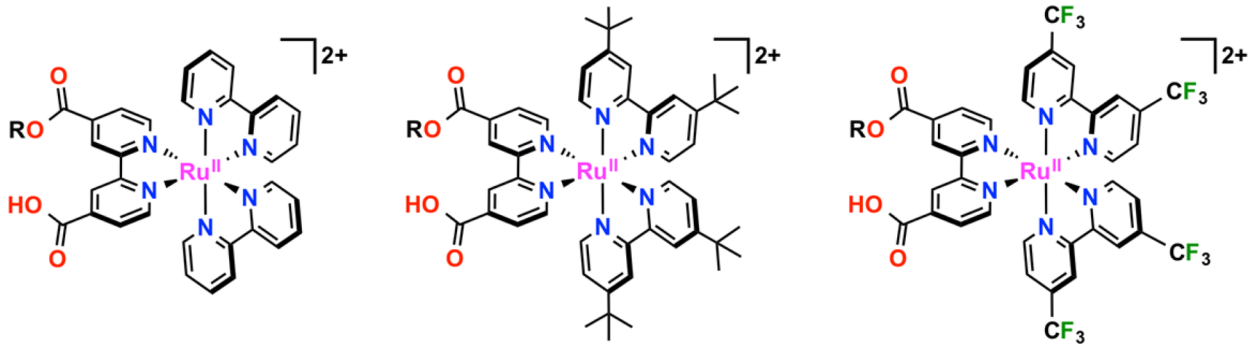

$[Ru(bpy)_2(mcb)]^{2+}$ (R = CH_2CH_3) $[Ru(dtb)_2(mcb)]^{2+}$ (R = CH_2CH_3) $[Ru(btfmb)_2(mcb)]^{2+}$ (R = CH_2CH_3)

$[Ru(bpy)_2(dcb)]^{2+}$ (R = H) $[Ru(dtb)_2(dcb)]^{2+}$ (R = H) $[Ru(btfmb)_2(dcb)]^{2+}$ (R = H)

Figure 1. Ruthenium polypyridyl compounds investigated herein.

always more acidic in the excited state than the ground state. Likewise, carboxylates are always more basic in their excited states. In other words, whether the acid ionization constant increases or decreases upon light absorption has always been solely determined by the identity of the functional group. Here we report the first exception to this rule. Carboxylic acid/carboxylate functional groups with almost identical ground state pK_a values can be made more acidic *or* more basic than the ground state in Ru(II) polypyridyl compounds.

Many literature reports of excited state acid−base chemistry in transition metal compounds have appeared since the first reports by Demas and Peterson[26] in 1976.[1,2,27−47] All known ruthenium polypyridine compounds with pendant carboxylates[30−34] or amines[35−37] were found to be photobases. Photoacidic ruthenium compounds are relatively rare and until now appear to be limited to phenol-type[28] or ambidentate cyanide ligands.[38] Most relevant to this manuscript are the studies of $[Ru(bpy)_2(dcb)]^{2+}$,[27] which is a weaker acid in the excited state than in the ground state, that is, a photobase. The presence of two carboxylic acid groups in $[Ru(bpy)_2(dcb)]^{2+}$ and the very similar absorption spectra of the mono- and diprotonated forms of this compound has led to significant discrepancy in the reported ionization constants.[27,32,33,48,49] This is unfortunate as the dcb ligand is commonly utilized for solar energy applications, such as in dye-sensitized solar cells.[50−52] The syntheses of model compounds and full wavelength spectral analysis reported herein have enabled accurate determination of the equilibrium constants and insights into their acid−base behavior.

The six ruthenium polypyridyl chromophores, presented in Figure 1, containing carboxylic acid substituted bipyridine ligands $[Ru^{II}(btfmb)_2(LL)]^{2+}$, $[Ru^{II}(dtb)_2(LL)]^{2+}$, and $[Ru^{II}(bpy)_2(LL)]^{2+}$, where bpy is 2,2′-bipyridine, btfmb is 4,4′-$(CF_3)_2$-bpy, and dtb is 4,4′-$((CH_3)_3C)_2$-bpy, and LL is either dcb or mcb = 4-(CO_2H),4′-(CO_2Et)-2,2′-bpy, were synthesized. All the compounds were similar ground state pK_a values; however, the btfmb compounds were found to be photoacids that rapidly equilibrate in the excited state; the other compounds were photobases that undergo excited state proton transfer equilibria on the nanosecond time scale as was quantified through time dependent photoluminescence spectral shifts and kinetic modeling.

EXPERIMENTAL SECTION

Materials. The following reagents were used as received from the following commercial suppliers: acetonitrile (Burdick metric grad); ethanol and *tert*-butanol (Fisher, certified); tetrahydrofuran (THF, Sigma-Aldrich, ACS grad); $RuCl_3{\cdot}3H_2O$ (Pressure Chemical); argon gas (Airgas, >99.998%); nitrogen gas (Airgas, 99.999%). Hydrochloric acid (HCl), ammonium hexafluorophosphate (NH_4PF_6), *n*-tetrabutylammonium hydroxide (TBAOH, 1.0 M in methanol), 4,4′-di-*tert*-butyl-2,2′-bipyridine (dtb), $AgNO_3$, $MgSO_4$, palladium(II) acetate ($Pd(OAc)_2$), K_2CO_3, NaOH, LiCl, 2-bromo-4-(trifluoromethyl)pyridine, tetrabutyl ammonium iodide (TBAI), and $[Ru(bpy)_3Cl_2{\cdot}6H_2O$ were purchased from Sigma-Aldrich and used as received. $Ru(bpy)_2Cl_2$, $Ru(dtb)_2Cl_2$, 4,4′-diethylester-2,2′-bipyridine (deeb), and [(p-cymene)Ru(deeb)Cl]Cl were prepared following a literature procedure.[53−56]

Synthesis. *4,4′-Ditrifluoromethyl-2,2′-bipyridine (btfmb).* The method of Kubiak et al.[57] was modified to synthesize this ligand first reported by Furue.[58] A mixture of 2-bromo-4-(trifluoromethyl)pyridine (1g, 4.4 mmol), $Pd(OAc)_2$ (50 mg, 0.22 mmol), TBAI (1.63 g, 4.4 mmol), K_2CO_3 (916 mg, 6.6 mmol), and *i*-PrOH (0.68 mL, 8.8 mmol) in 15 mL of DMF was heated at 100 °C for 20 h. The heating was suspended, and the reaction mixture was filtered through a fine frit. Then 50 mL of DCM was added to the filtrate and was washed with deionized water (50 mL × 3). The organic layer was collected, and the water layer was further extracted with 20 mL of DCM. The combined organic layer was dried with anhydrous $MgSO_4$, and concentrated to dryness on rotary evaporator. The crude was dissolved in 2 mL of DCM, and loaded onto a silica gel column (4 cm × 15 cm) using hexane/ethyl acetate (v:v = 10:1) as eluent. The first colorless band was collected and concentrated to dryness to afford 520 mg of white solid as product. (Yield = 81%.) ^{1}H NMR (400 MHz, $CDCl_3$) δ 8.88 (d, J = 5.0 Hz, 2H), 8.73 (s, 2H), 7.59 (d, J = 4.9 Hz, 2H). ^{13}C NMR (101 MHz, $CDCl_3$) δ 156.23, 150.42, 139.92, 139.58, 124.33, 121.62, 120.11, 120.07, 120.04, 120.00, 117.34, 117.31, 117.27, 117.23.

4-Ethylester-4′-carboxy-2,2′-bipyridine (mcb). The deeb ligand (1 g, 3.3 mmol) was dissolved in 100 mL of THF. To the mixture, 40 mL of EtOH and 5 mL of aqueous solution of NaOH (200 mg, 5 mmol) were added sequentially. The mixture was purged with Ar for 30 min and allowed to stir at RT for 24 h. The solvent was removed on a rotary evaporator, and the crude was redissolved in 30 mL of deionized water. An amount of 830 mg of unreacted deeb was recovered by filtration through a medium frit. HCl (1 M) was added dropwise to the filtrate to adjust pH = 3.8, at which point a large amount of white solid precipitated out of the solution. The suspension was filtered through a medium frit and then rinsed with water (pH = 3.8). The filter cake was dried in vacuum oven to afford 147 mg of white solid product. (Yield = 94%.) ^{1}H NMR (400 MHz, DMSO-d_6) δ 13.84 (s, br, 1H), 8.93 (t, J = 5.2 Hz, 2H), 8.84 (s, 2H), 7.93 (td, J = 5.4, 1.6 Hz, 2H), 4.42 (q, J = 7.1 Hz, 2H), 1.38 (t, J = 7.1 Hz, 3H). ^{13}C NMR (101 MHz, DMSO-d_6) δ 165.99, 164.49, 155.60, 155.34, 150.82, 150.69, 138.50, 123.59, 123.27, 119.59, 119.18, 61.81, 14.07.

Ru(btfmb)$_2$Cl$_2$. A mixture of $RuCl_3{\cdot}3H_2O$ (225 mg, 0.86 mmol), btfmb (500 mg, 1.71 mmol), and predried LiCl (220 mg, 5.2 mmol) in 10 mL of DMF was purged with Ar for 20 min, and was heated at reflux for 12 h under Ar atmosphere. DMF was removed on a rotary

DOI: 10.1021/jacs.6b00454
J. Am. Chem. Soc. 2016, 138, 3891−3903

evaporator, and the crude product was extracted with DCM to remove LiCl. DCM was removed on a rotary evaporator, and the obtained solid was redissolved in minimum amount of DCM and loaded onto a silica gel column (4 cm × 20 cm) using DCM/hexane (v:v = 2:1) as eluent. After removing a fast moving light yellow band, the eluent was changed to DCM/ethyl acetate (v:v = 2:1), and the dark green band was collected, concentrated to dryness in vacuo to afford 450 mg of black solid as product. (Yield = 69%.) ^{1}H NMR (400 MHz, acetone-d_6) δ 10.44 (d, J = 6.0 Hz, 2H), 9.21 (d, J = 2.0 Hz, 2H), 9.06 (d, J = 1.9 Hz, 2H), 8.20 (d, J = 6.1 Hz, 2H), 8.14 (dd, J = 6.0, 1.9 Hz, 2H), 7.43 (dd, J = 6.1, 1.9 Hz, 2H). ^{13}C NMR (101 MHz, acetone-d_6) δ 206.18, 161.84, 160.06, 156.09, 155.06, 136.77, 136.43, 135.55, 135.21, 125.47, 125.17, 122.76, 122.24, 122.21, 121.96, 120.67, 120.63, 120.60, 120.56, 120.32, 120.28.

[Ru(bpy)$_2$(deeb)](PF$_6$)$_2$. A mixture of Ru(bpy)$_2$Cl$_2$ (242 mg, 0.50 mmol), deeb (160 mg, 0.53 mmol), and 15 mL of EtOH in a 25 mL microwave vessel was purged with Ar for 20 min, and was heated at 130 °C for 30 min in Anton Parr microwave reactor. The solvent was removed on a rotary evaporator, and the reaction mixture was redissolved in 10 mL of deionized water. The solution was filtered through a fine frit to remove excess of deeb. An amount of 326 mg NH_4PF_6 (2 mmol) in 2 mL of deionized water was added to the filtrate to form a dark orange solid precipitate. The suspension was allowed to stir vigorously at RT for 15 min followed by filtering through a fine frit. The filter cake was rinsed with 30 mL of deionized water and dried in vacuum oven to afford 370 mg of dark orange solid. (Yield = 74%.) ^{1}H NMR (400 MHz, CD_3CN-d_3) δ 9.03 (dd, J = 1.9, 0.7 Hz, 2H), 8.50 (ddt, J = 8.1, 4.2, 1.1 Hz, 4H), 8.08 (qd, J = 7.6, 1.5 Hz, 4H), 7.94 (dd, J = 5.8, 0.7 Hz, 2H), 7.82 (dd, J = 5.9, 1.7 Hz, 2H), 7.70 (ddd, J = 5.6, 1.5, 0.7 Hz, 2H), 7.66 (ddd, J = 5.6, 1.5, 0.7 Hz, 2H), 7.42 (ddd, J = 7.6, 5.6, 1.3 Hz, 2H), 7.38 (ddd, J = 7.7, 5.6, 1.3 Hz, 2H), 4.46 (q, J = 7.1 Hz, 4H), 1.41 (t, J = 7.1 Hz, 6H). ^{13}C NMR (101 MHz, CD_3CN-d_3) δ 164.40, 158.68, 157.71, 157.59, 153.81, 152.78, 152.54, 139.79, 139.24, 128.74, 128.65, 127.42, 125.38, 124.59, 63.62, 14.39. HR-ESI-MS: m/z = 343.0615 (calcd. for $[RuC_{34}H_{28}N_6O_4]^{2+}$ ($[Ru(bpy)_2(dcb) - C_2H_4]^{2+}$): 342.8521).

[Ru(dtb)$_2$(deeb)](PF$_6$)$_2$. A mixture of [(p-cymene)Ru(deeb)Cl]Cl (606 mg, 1 mmol), 4,4-di-*tert*-butyl-2,2′-bipyridine (dtb, 540 mg, 2 mmol), and $AgNO_3$ (375 mg, 2.2 mmol) in 30 mL of EtOH was purged with Ar for 20 min, and was heated at reflux for 8 h. The reaction mixture was condensed to 10 mL and filtered through a fine frit to remove AgCl. NH_4PF_6 (500 mg, 3 mmol) in 2 mL of deionized water was added to the filtrate to form a dark orange precipitate. The suspension was allowed to stir at RT for 15 min, followed by filtering through a fine frit. The obtained filter cake was dried in vacuo and recrystallized from DCM/ether to afford 1 g of dark orange solid as product. (Yield = 81%.) ^{1}H NMR (400 MHz, CD_3CN-d_6) δ 9.02 (d, J = 1.0 Hz, 2H), 8.48 (dd, J = 7.1, 2.0 Hz, 4H), 7.90 (d, J = 5.9 Hz, 2H), 7.83 (dd, J = 5.8, 1.7 Hz, 2H), 7.52 (dd, J = 9.9, 6.0 Hz, 4H), 7.42 (dd, J = 6.0, 2.0 Hz, 2H), 7.34 (dd, J = 6.0, 2.0 Hz, 2H), 4.46 (q, J = 7.1 Hz, 4H), 1.44−1.36 (m, 42H). ^{13}C NMR (400 MHz, CD_3CN-d_6) δ 164.5, 164.0, 158.8, 157.5, 153.5, 152.0, 151.6, 139.4, 127.3, 125.69, 125.6, 124.4, 122.6, 73.1, 63.6, 36.3, 30.4, 14.4. HR-ESI-MS: m/z = 1083.3638 (calcd. for $[C_{52}H_{64}N_6O_4PF_6]^+$ ($[Ru(dtb)_2(deeb)](PF_6)^+$): 1083.1521); m/z = 469.2004 (calcd. for $[C_{52}H_{64}N_6O_4]^{2+}$ ($[Ru(dtb)_2(deeb)]^{2+}$): 469.0940).

[Ru(btfmb)$_2$(deeb)](PF$_6$)$_2$. A mixture of Ru(btfmb)$_2$Cl$_2$ (120 mg, 0.16 mmol), deeb (48 mg, 0.16 mmol), $AgNO_3$ (60 mg, 0.35 mmol), and 14 mL of EtOH in a 25 mL microwave vessel was purged with Ar for 20 min, and was heated at 160 °C for 1 h in an Anton Parr microwave reactor. AgCl was removed by filtering through a fine frit, and 100 mg (0.61 mmol) of NH_4PF_6 in 2 mL of deionized water was added to the filtrate to form an orange precipitate. The suspension was allowed to stir at RT for 15 min, followed by filtering through a fine frit. The filter cake was rinsed with water and ethanol sequentially, and dried in vacuum oven to afford 174 mg of orange solid as product. (Yield = 86%.) ^{1}H NMR (400 MHz, CD_3CN-d_3) δ 9.07 (d, J = 1.7 Hz, 2H), 8.95 (s, 4H), 7.98 (d, J = 5.9 Hz, 2H), 7.93 (d, J = 5.9 Hz, 2H), 7.89 (d, J = 5.8 Hz, 2H), 7.85 (dd, J = 5.8, 1.7 Hz, 2H), 7.70 (ddd, J = 12.6, 5.9, 1.9 Hz, 4H), 4.47 (q, J = 7.1 Hz, 4H), 1.41 (t, J = 7.1 Hz, 6H). ^{13}C NMR (101 MHz, CD_3CN-d_3) δ 164.26, 158.36, 158.28, 158.17, 154.99, 154.76, 154.36, 140.97, 140.29, 139.96, 127.79, 125.12, 124.98, 122.67, 63.78, 14.38. HR-ESI-MS: m/z = 479.0371 (calcd. for $[RuC_{38}H_{24}N_6O_4F_{12}]^{2+}$ ($[Ru(btfmb)_2(dcb) - C_2H_4]^{2+}$): 478.8486).

[Ru(bpy)$_2$(dcb)](PF$_6$)$_2$. [Ru(bpy)$_2$(deeb)](PF$_6$)$_2$ (170 mg, 0.17 mmol) was dissolved in 15 mL of acetone, and 5 mL of 0.5 M aqueous NaOH solution was added. The mixture was purged with Ar for 15 min and was heated at 55 °C overnight. Acetone was removed on a rotary evaporator, and 1 M HPF_6 aqueous solution was added to the solution to adjust the pH = 1, causing dark orange precipitate, which was collected by filtration through a fine frit, rinsed with deionized water, and dried in vacuum oven to afford 135 mg of product. (Yield = 84%.) ^{1}H NMR (400 MHz, CD_3CN-d_3) δ 9.09 (s, 2H), 8.50 (dd, J = 8.2, 3.8 Hz, 4H), 8.12−8.03 (m, 4H), 7.92 (d, J = 5.8 Hz, 2H), 7.82 (dd, J = 5.8, 1.7 Hz, 2H), 7.70 (dd, J = 5.7, 1.3 Hz, 2H), 7.67−7.64 (m, 2H), 7.42 (ddd, J = 7.2, 5.7, 1.3 Hz, 2H), 7.38 (ddd, J = 7.2, 5.6, 1.3 Hz, 2H). ^{13}C NMR (101 MHz, CD_3CN-d_3) δ 165.00, 158.65, 157.72, 157.60, 153.72, 152.76, 152.53, 139.90, 139.22, 128.73, 128.66, 127.71, 125.37, 124.90.

[Ru(dtb)$_2$(dcb)](PF$_6$)$_2$. A mixture of [Ru(deeb) (dtb)$_2$](PF$_6$)$_2$ (400 mg, 0.33 mmol), and 5 mL of 0.5 M aqueous NaOH solution in 30 mL of acetone was purged with N_2 for 15 min and was heated at 55 °C for 12 h. The reaction mixture was filtered through a fine frit and rinsed with 10 mL of deionized water. Acetone was removed from the filtrate on rotary evaporator, and 30 mL of deionized water was added to dissolve the crude product. To this solution HPF_6 (1 M) was added dropwise to adjust the pH = 1 to form an orange brown precipitate. The precipitate was collected on a fine frit by filtration, rinsed with deionized water and dried in vacuum oven affording 330 mg of product. (Yield = 85%.) ^{1}H NMR (400 MHz, CD_3CN-d_3) δ 9.02 (s, 2H), 8.48 (dd, J = 6.6, 2.0 Hz, 4H), 7.90 (d, J = 5.9 Hz, 2H), 7.83 (dd, J = 5.8, 1.6 Hz, 2H), 7.53 (dd, J = 10.9, 6.1 Hz, 4H), 7.43 (dd, J = 6.1, 1.9 Hz, 2H), 7.35 (dd, J = 6.1, 2.0 Hz, 2H), 1.42 (2, 18H), 1.39 (2, 18H). ^{13}C NMR (101 MHz, CD_3CN-d_3) δ 166.1, 163.8, 158.9, 157.5, 157.5, 153.1, 152.8, 152.0, 151.6, 127.6, 125.7, 125.6, 124.9, 122.5, 36.3, 30.41. HR-ESI-MS: m/z = 1027.3028 (calcd. for $[RuC_{48}H_{56}N_6O_4PF_6]^+$ ($[Ru(dtb)_2(dcb)(PF_6)]^+$): 1027.0446); m/z = 441.1691 (calcd. for $[RuC_{48}H_{56}N_6O_4]^{2+}$ ($[Ru(dtb)_2(dcb)]^{2+}$): 441.0402).

[Ru(btfmb)$_2$(dcb)](PF$_6$)$_2$. A mixture of Ru(btfmb)$_2$(deeb) (PF$_6$)$_2$ (110 mg, 0.086 mmol), Et_3N (0.5 mL), H_2O (1 mL), and acetone (5 mL) was purged with Ar for 20 min, and was then heated at 55 °C overnight. After that the solvent was removed on a rotary evaporator, and the crude was redissolved in 5 mL of deionized water. To the mixture, 1 M HPF_6 aqueous solution was added to tune the pH = 1 causing an orange precipitate, which was collected on a fine frit, followed by rinsing with water and drying in vacuo to afford 96 mg of product. (Yield = 92%.) ^{1}H NMR (400 MHz, D_2O) δ 9.02 (d, J = 3.8 Hz, 4H), 8.93 (s, 2H), 8.10 (dd, J = 12.1, 5.9 Hz, 4H), 7.86−7.77 (m, 6H), 7.74 (dd, J = 5.9, 1.6 Hz, 2H). ^{13}C NMR (101 MHz, D_2O) δ 171.23, 158.11, 157.98, 157.62, 153.74, 153.67, 152.42, 147.14, 139.87, 139.52, 127.12, 124.61, 124.17, 123.93, 122.06, 121.21. HR-ESI-MS: m/z = 465.0214 (calcd. for $[RuC_{36}H_{20}N_6O_4F_{12}]^{2+}$ ($[Ru(btfmb)_2(dcb)]^{2+}$): 464.8217.

[Ru(bpy)$_2$(mcb)](PF$_6$)$_2$. Ru(bpy)$_2$Cl$_2$ (70 mg, 0.15 mmol), mcb (40 mg, 0.15 mmol) and 6 mL EtOH was added into a 10 mL microwave vessel. The mixture was purged with Ar for 20 min and was heated at 140 °C for 45 min in an Anton Parr microwave reactor. The solvent was removed on rotary evaporator, and the crude product was redissolved in ∼5 mL of deionized water. The solution was filtered through a fine frit to remove unreacted starting materials. An mount of 95 mg of NH_4PF_6 (0.6 mmol) in 1 mL of water was added to the filtrate to create an orange suspension. The mixture was stirred at RT for 15 min followed by filtering through a medium frit. The filter cake was rinsed with deionized water and dried in vacuum oven affording 100 mg of orange solid as product. (Yield = 71%.) ^{1}H NMR (400 MHz, CD_3CN-d_3) δ 9.05 (d, J = 1.6 Hz, 1H), 9.00 (d, J = 1.7 Hz, 1H), 8.50 (dt, J = 7.0, 2.9 Hz, 4H), 8.14−7.99 (m, 4H), 7.93 (d, J = 5.9 Hz, 1H), 7.89 (d, J = 5.8 Hz, 1H), 7.84 (dd, J = 5.8, 1.6 Hz, 1H), 7.80 (dd, J = 5.8, 1.7 Hz, 1H), 7.70 (d, J = 5.6 Hz, 2H), 7.67 (t, J = 5.9 Hz, 2H), 7.45−7.34 (m, 4H), 4.44 (q, J = 7.1 Hz, 2H), 1.40 (t, J = 7.1 Hz, 3H). ^{13}C NMR (101 MHz, CD_3CN-d_3) δ 164.44, 157.74, 157.66, 153.74, 153.46, 152.76, 152.55, 139.72, 139.16, 128.70, 128.65, 127.90, 127.26, 125.34, 124.94, 124.42, 63.59, 30.84, 14.38. HR-ESI-MS: m/z = 685.1113 (calcd. for $[RuC_{34}H_{27}N_6O_4]^+$

DOI: 10.1021/jacs.6b00454
J. Am. Chem. Soc. 2016, 138, 3891−3903

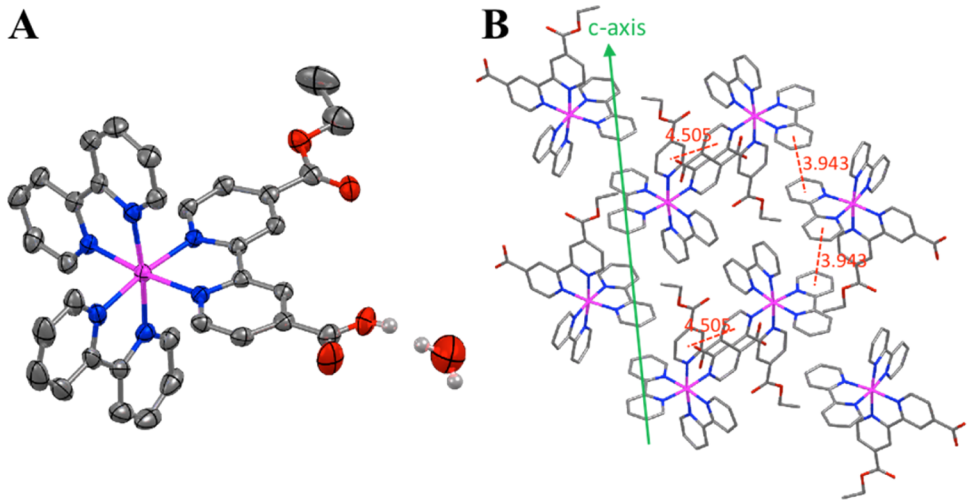

Figure 2. (A) Crystal structure of $[Ru(bpy)_2(mcb)](PF_6)_2$. Thermal ellipsoids at the 50% probability level. Anions and all hydrogen atoms are omitted for clarity purpose except for the ones on the carboxylic acid group and water molecule. Color code: Pink, Ru; blue, N; red, O; gray, C; light gray, H. (B) Crystal packing along *c*-axis; the red dashed lines represent the centroid distances between two stacked pyridine rings.

($[Ru(bpy)_2(mcb) - H]^+$): 684.6962); m/z = 343.0599 (calcd. for $[RuC_{34}H_{28}N_6O_4]^{2+}$ ($[Ru(bpy)_2(mcb)]^{2+}$): 342.8521).

[Ru(dtb)$_2$(mcb)](PF$_6$)$_2$. A mixture of $Ru(dtb)_2Cl_2$ (104 mg, 0.15 mmol), mcb (40 mg, 0.15 mmol), and 6 mL of EtOH in a 10 mL microwave vessel was purged with Ar for 20 min and was heated at 140 °C for 45 min in an Anton Parr microwave reactor. The solvent was condensed to ~5 mL, and 95 mg of NH_4PF_6 (0.58 mmol) in 2 mL of deionized water was added to form an orange brown precipitate. The mixture was allowed to stir at RT for 15 min, followed by filtering through a medium frit. The filter cake was dried in a vacuum oven, and was then recrystallized in acetone/diethyl ether twice to afford 80 mg of product as an orange-brown solid. (Yield = 50%.) ^{1}H NMR (400 MHz, CD_3CN-d_3) δ 9.04 (s, 1H), 9.00 (s, 1H), 8.47 (dd, J = 6.2, 3.0 Hz, 4H), 7.93−7.78 (m, 4H), 7.59−7.48 (m, 4H), 7.42 (dd, J = 6.2, 2.0 Hz, 2H), 7.34 (d, J = 6.0 Hz, 2H), 4.45 (q, J = 7.1 Hz, 2H), 1.44−1.37 (m, 39H). ^{13}C NMR (101 MHz, CD_3CN-d_3) δ 164.51, 163.96, 159.04, 158.47, 157.53, 157.44, 153.42, 153.17, 152.01, 151.60, 139.30, 127.78, 127.17, 125.71, 125.63, 124.81, 124.29, 122.58, 63.56, 36.32, 30.42, 14.39. HR-ESI-MS: m/z = 909.3626 (calcd. for $[RuC_{50}H_{59}N_6O_4]^+$ ($[Ru(dtb)_2(mcb) - H]^+$): 909.1263); m/z = 455.1848 (calcd. for $[RuC_{50}H_{60}N_6O_4]^{2+}$ ($[Ru(dtb)_2(mcb)]^{2+}$): 455.0671).

[Ru(btfmb)$_2$(mcb)](NO$_3$)$_2$. A mixture of $Ru(btfmb)_2Cl_2$ (168 mg, 0.22 mmol), mcb (60 mg, 0.22 mmol), $AgNO_3$ (45 mg, 0.27 mmol), and 10 mL lf EtOH in a 25 mL microwave vessel was purged with Ar for 20 min, and was then heated at 140 °C for 2 h in an Anton Parr microwave reactor. AgCl was removed by by filtering through a fine frit, and the filtrate was concentrated to drynss on rotary evaporator. A volume of 100 mL of DCM was added to the crude to extract the impurity. The DCM solution was separated from the undissolved orange solid, condensed to ~20 mL, and placed in a freezer overnight. The orange solid that precipitated out from DCM solution was combined with the original undissolved solid. The combined solid was dissolved in 5 mL of acetone, and excess $AgNO_3$ was removed by filtration. The filtrate was recrystallized in acetone/ether twice to afford 120 mg of red-orange solid as product. (Yield = 50%.) ^{1}H NMR (400 MHz, methanol-d_4) δ 9.36 (s, 4H), 9.17−9.08 (m, 2H), 8.15 (t, J = 5.8 Hz, 2H), 8.12 (d, J = 6.0 Hz, 1H), 8.08 (d, J = 6.0 Hz, 1H), 8.02 (d, J = 5.8 Hz, 1H), 7.96 (dd, J = 5.8, 1.7 Hz, 1H), 7.91−7.80 (m, 6H), 4.51 (q, J = 7.1 Hz, 2H), 1.44 (t, J = 7.1 Hz, 3H). ^{13}C NMR (101 MHz, CD_3OD-d_4) δ 164.48, 159.36, 159.26, 159.22, 159.17, 157.60, 154.88, 154.75, 154.61, 154.05, 153.24, 141.24, 141.13, 140.78, 128.88, 127.85, 125.63, 125.37, 124.77, 123.13, 122.22, 63.93, 14.46. HR-ESI-MS: m/z = 479.0373 (calcd. for $[RuC_{38}H_{24}N_6O_4F_{12}]^{2+}$ ($[Ru(btfmb)_2(mcb)]^{2+}$): 478.8486).

Spectroscopy. *UV−Visible Absorption.* UV−visible absorption spectra were obtained on a Varian Cary 50 or an Agilent Cary 60 spectrophotometer at room temperature in 1.0 cm path length quartz cuvettes. Unless otherwise specified, the solutions were bubbled with argon gas for >30 min prior to photoluminescence and transient absorption studies. The pH dependent absorption and PL spectra were obtained from pH 1 to 14. The pH was monitored in situ with an Oakton pH 11 m (Cole Parmer).

Steady-State Photoluminescence. Steady spectra were obtained with a HORIBA Fluorolog spectrophotometer equipped with a 450 W Xe arc lamp for the excitation source. PL spectra were obtained at room temperature with PL detected at a right angle to the excitation beam. Quantum yields were measured versus $[Ru(bpy)_3]Cl_2$ in water as the standard (ϕ_{PL} = 0.042) with the optically dilute method.[59]

Time-Resolved Experiments. Nanosecond transient absorption measurements were obtained with an apparatus similar to that which has been previously described. Briefly, samples were excited by a Q-switched, pulsed Nd:YAG laser (Quantel U.S.A. (BigSky) Brilliant B; 5−6 ns full width at half-maximum (fwhm), 1 Hz, ~10 mm in diameter) tuned to 532 nm with the appropriate nonlinear optics. The excitation fluence was measured with a thermopile power meter (Molectron) that was typically 3−5 mJ/pulse. A 150 W Xe arc lamp served as the probe beam and was aligned orthogonal to the laser excitation light. The probe lamp was pulsed for measurements on sub-100 μs time scales. Detection was achieved with a monochromator (SPEX 1702/04) optically coupled to an R928 photomultiplier tube (Hamamatsu). Transient data was acquired with a computer-interfaced digital oscilloscope (LeCroy 9450, Dual 330 MHz) with an overall instrument response time of ~10 ns. Typically, 30 laser pulses were averaged at each observation wavelength over the range 340−750 at 10 nm intervals. Full spectra were generated by averaging 2−10 points on either side of the desired time value to reduce noise in the raw data. Time-resolved photoluminescence was obtained using the same experimental setup described above with the exception of the Xe arc lamp as the probe beam. PL signals were acquired at a right angle to excitation with pulsed 532 nm laser light, and fluence was typically 1 mJ/pulse. Typically, 300 laser shots were averaged and digitized on a computer-interfaced oscilloscope.

RESULTS

The six ruthenium polypyridyl compounds shown in Figure 1 were synthesized in high yield. The dcb containing compounds with dtb or bpy have been previously reported.[27,60] The compounds with one ethyl ester group and one carboxylic acid group were newly synthesized. Crystals of $[Ru(bpy)_2(mcb)]^{2+}$ suitable for single crystal diffraction studies were obtained and the refined structure is shown in Figure 2.

Each mcb ligand clearly possessed one ethyl ester group and one carboxylic acid group in the *para* position of each pyridine

DOI: 10.1021/jacs.6b00454
J. Am. Chem. Soc. 2016, 138, 3891−3903

ring. The carboxylic acid group formed a hydrogen bond with a nearby water molecule as is shown. The average Ru−N distance was 2.57 Å with a 79.2° average bite angle for the three ligands. Crystal packing propagates along the *c*-axis through $\pi-\pi$ interactions with a centroid distance of 3.94 Å between the pyridine rings.[61] Each Ru compound also showed evidence for weaker $\pi-\pi$ interactions between the mcb ligands, with an interlayer distance of 4.51 Å. The detailed crystal structure information is given in Table 1.

Table 1. Crystallographic Data and Structure Refinement for $[Ru(bpy)_2(mcb)](PF_6)_2$

empirical formula	$C_{34}H_{30}F_{12}N_6O_5P_2Ru$
formula weight	993.65
temperature/K	100
crystal system	monoclinic
space group	P21/c
a/Å	11.8405(3)
b/Å	24.0489(6)
c/Å	13.5875(4)
α/deg	90
β/deg	98.2170(17)
γ/deg	90
volume/Å^3	3829.33(18)
Z	4
ρ_{calc}g/cm^3	1.724
μ/mm^{-1}	5.105
crystal size/mm^3	0.219 × 0.129 × 0.071
radiation	Cu Kα (λ = 1.54178)
Final *R* indexes [$I \geq 2\sigma$ (I)]	*R*1 = 0.0516, *wR*2 = 0.1266
final *R* indexes [all data]	*R*1 = 0.0576, *wR*2 = 0.1302

All the ruthenium polypyridyl compounds displayed broad metal-to-ligand charge transfer (MLCT) absorption bands centered at ∼460 nm when dissolved in water with pH greater than 5.5. Titration with HCl led to significant changes in the visible absorption spectra with maintenance of isosbestic points. Representative data for $[Ru(dtb)_2(dcb)]^{2+}$ and $[Ru(btfmb)_2(dcb)]^{2+}$ are given in Figure 3. At pH values less than 3, $[Ru^{II}(btfmb)_2(dcb)]^{2+}$ displayed sharper and more intense absorption than in alkaline solution while $[Ru^{II}(dtb)_2(dcb)]^{2+}$ exhibited two distinct MLCT absorption bands, with maxima at 430 and 480 nm, and a decreased absorptivity at 450 nm. Titration of the mcb compounds enabled the spectroscopic identification of the intermediate, monoprotonated, state of all the dcb compounds, $[RuL_2(dcb)]^{1+}$, via direct spectral comparison, Figure S1 (Supporting Information). Shown in black in Figure 3 are the absorption spectra of the monoprotonated compounds that have absorption spectra that are very similar to that of the mcb compounds. The absorbance for all compounds was pH independent over the ranges pH 5−12 and pH 1−2.

Visible light excitation resulted in room temperature photoluminescence (PL) for all the compounds. Under basic conditions, $[Ru^{II}(btfmb)_2(dcb)]^{2+*}$ exhibited PL centered at 648 nm that blue-shifted to 633 nm in acidic solution; an energy increase of approximately 370 cm^{-1}. The PL from $[Ru^{II}(dtb)_2(dcb)]^{2+*}$ dissolved in basic aqueous solution displayed a maximum at 653 nm that red-shifted to 693 nm under acidic conditions; an approximately 950 cm^{-1} energetic shift. The PL spectra measured under highly acidic and basic conditions were assigned as the protonated and deprotonated form of the compounds, respectively. For all compounds the PL intensity increased as the spectra shifted toward shorter wavelength, Table 2. Titration of the mcb compounds afforded knowledge of the PL spectra for the monoprotonated states of the dcb compounds, Figure S1. The corrected PL spectra were modeled with a Franck−Condon line-shape analysis that afforded the E_{00} value as has been previously reported.[62,63]

The PL quantum yields ϕ_{PL}, expressed as a percentage ranged from 0.33% to 5.23%, Table 2. Pulsed light excitation of the compounds in aqueous solutions with pH < 2 or pH > 5.5 yielded excited states that decayed to the ground state by a first-order kinetic process with characteristic excited state lifetimes, $\tau_{obs} = 1/k_{obs}$. Knowledge of ϕ_{PL} and k_{obs} enabled calculation of the radiative, k_r, and nonradiative, k_{nr}, decay rate constants, eq 3.

$$k_r = \eta\phi_{PL}k_{obs}; \quad k_{nr} = k_{obs} - k_r \tag{3}$$

where η is the intersystem crossing quantum yield and is assumed to be 1 as found for $[Ru(bpy)_3]^{2+}$.[51,64,65] A plot of the nonradiative rate constants versus the E_{00} energy for all compounds was found to be linear as predicted by the energy gap law, Figure S2. The photophysical parameters are given in Table 2. At intermediate pH values where an excited state acid−base equilibrium was relevant for the photobasic compounds, PL

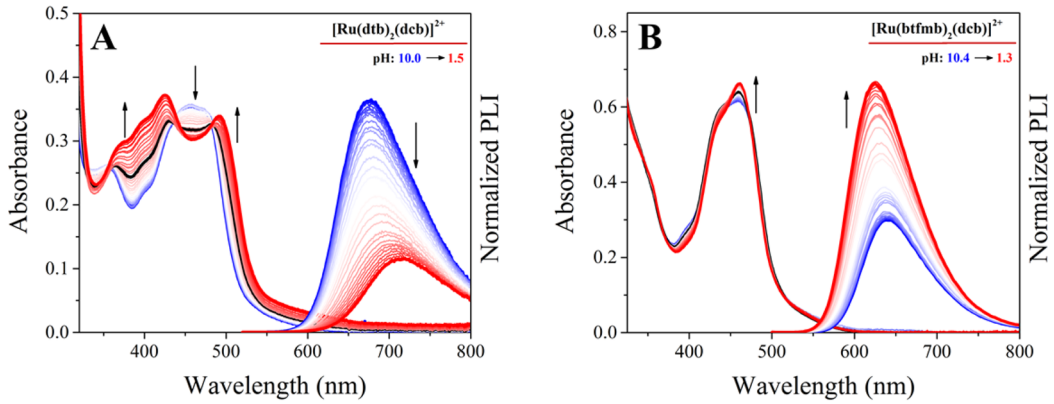

Figure 3. Visible absorption and photoluminescence spectra of $[Ru(dtb)_2(dcb)]^{2+}$ (A) and $[Ru(btfmb)_2(dcb)]^{2+}$ (B) in aqueous solution over the indicated pH range. The arrows indicate the spectral changes measured as the pH was decreased by titration with HCl. The spectra in bold blue are assigned to the fully deprotonated carboxylate compounds, while the bold black are the monoprotonated compound, and the bold red are assigned to the diprotonated carboxylic acid form of the compounds.

DOI: 10.1021/jacs.6b00454
J. Am. Chem. Soc. 2016, 138, 3891−3903

Table 2. Photophysical Properties in Acidic and Basic Aqueous Solution

compd	pH[a]	MLCT (nm)[b]	PL_{max} (nm)[b]	ϕ_{PL} (%)[c]	τ (ns)[cd]	k_r (s^{-1})[e]	k_{nr} (s^{-1})[f]
$[Ru(bpy)_2(mcb)]^{2+}$	6.3	472	679	2.1	340	6.2×10^4	2.9×10^6
	1.6	479	694	1.5	270	5.6×10^4	3.6×10^6
$[Ru(dtb)_2(mcb)]^{2+}$	7.3	483	701	0.53	210	2.5×10^4	4.8×10^6
	1.6	593	720	0.38	150	2.5×10^4	6.6×10^6
$[Ru(btfmb)_2(mcb)]^{2+}$	4.5	459	640	3.9	550	7.1×10^4	1.7×10^6
	1.5	460	635	5.9	670	7.7×10^4	1.4×10^6
$[Ru(bpy)_2(dcb)]^{2+}$	10.5	459	653	3.9	530	7.3×10^4	1.8×10^6
	1.0	481	693	1.5	260	5.7×10^4	3.8×10^6
$[Ru(dtb)_2(dcb)]^{2+}$	10.0	455	676	1.3	300	4.2×10^4	3.3×10^6
	1.5	493	715	0.33	140	2.4×10^4	7.1×10^6
$[Ru(btfmb)_2(dcb)]^{2+}$	10.5	460	648	2.6	440	5.8×10^4	2.2×10^6
	0.4	460	633	5.2	690	7.6×10^4	1.4×10^6

[a]Aqueous solutions. [b]Wavelengths are ±2 nm. [c]PL quantum yields measured using $[Ru(bpy)_3]Cl_2$ in water as a standard (ϕ_{PL} = 0.042) with errors of ±10%.[59] [d]Lifetimes are ±5%. [e]$k_r = \eta\phi_{PL}k_{obs}$. [f]$k_{nr} = k_{obs} - k_r$. All measurements were obtained at +20 °C ± 2 °C.

Table 3. Ground and Excited State pK_a for All Compounds Containing the mcb Ligand

	pK_a		pK_a*		
compd	inflection point[a]	spectral modeling[b]	Förster cycle[c]	lifetime[d]	spectral modeling[e]
$[Ru(bpy)_2(mcb)]^{2+}$	2.31	2.31	3.08	2.77[f]	2.95
$[Ru(dtb)_2(mcb)]^{2+}$	2.51	2.38	3.23	3.18[f]	3.35
$[Ru(btfmb)_2(mcb)]^{2+}$	2.25	2.24	1.88	2.08	2.02

[a]Calculated from the inflection point of the spectrophotometric titration curve, Figure S3. [b]Calculated from spectral modeling of the UV−vis absorption data, Figure 4. [c]Calculated with eq 8. [d]Calculated with eq 7. [e]Calculated from the spectral modeling of PL titration data. [f]Assumptions for lifetime correction were not justified for these excited states, see Discussion.

Table 4. Ground and Excited State pK_a for All Compounds Containing the dcb Ligand

	inflection point	spectral modeling		Förster cycle		lifetime		spectral modeling	
compd	pK_a[a]	pK_{a1}[b]	pK_{a2}[b]	pK_{a1}*[c]	pK_{a2}*[c]	pK_{a1}*[d]	pK_{a2}*[d]	pK_{a1}*[e]	pK_{a2}*[e]
$[Ru(bpy)_2(dcb)]^{2+}$	2.55	2.01	2.83	2.78	4.07	2.58[f]	3.72[f]	2.70	3.90
$[Ru(dtb)_2(dcb)]^{2+}$	2.91	2.15	3.15	3.00	4.32	2.65[f]	3.93[f]	2.94	4.06
$[Ru(btfmb)_2(dcb)]^{2+}$	2.89	2.20	3.15	1.84	2.72	1.48	2.19	1.43	2.15

[a]Calculated from the inflection point of the *raw* spectrophotometric titration curve, Figure S4. [b]Calculated from spectral modeling of the UV−vis absorption data, Figure 5. [c]Calculated with eq 8. [d]Calculated with eq 7. [e]Calculated from spectral modeling of the PL data and appropriated corrections to the PL quantum yield. [f]Assumptions for lifetime correction were not justified for these excited states, see Discussion.

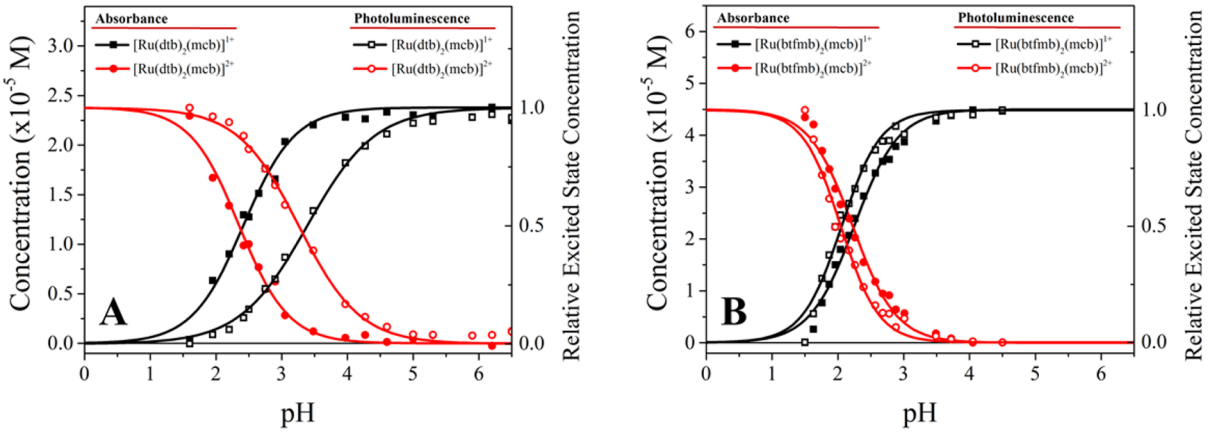

Figure 4. Spectral modeling curves of $[Ru(dtb)_2(mcb)]^{2+}$ (A) and $[Ru(btfmb)_2(mcb)]^{2+}$ (B) reporting on the ground state concentration (solid symbols) and relative excited state concentration (open symbols) changes of the indicated protonation states as a function of the pH.

decays monitored at all observation wavelengths were no longer single exponential and were instead well described by a biexponential kinetic model.

The ground-state pK_a's were determined from inflection points in the spectrophotometric titration data monitored at single wavelengths, Figures S3 and S4, as well as by full wavelength spectral modeling since the pH value where equal concentrations of the acid and conjugated base defines the pK_a, Tables 3 and 4. Representative spectral analysis data for monocarboxylic acid compounds and for dicarboxylic acid

DOI: 10.1021/jacs.6b00454
J. Am. Chem. Soc. 2016, 138, 3891−3903

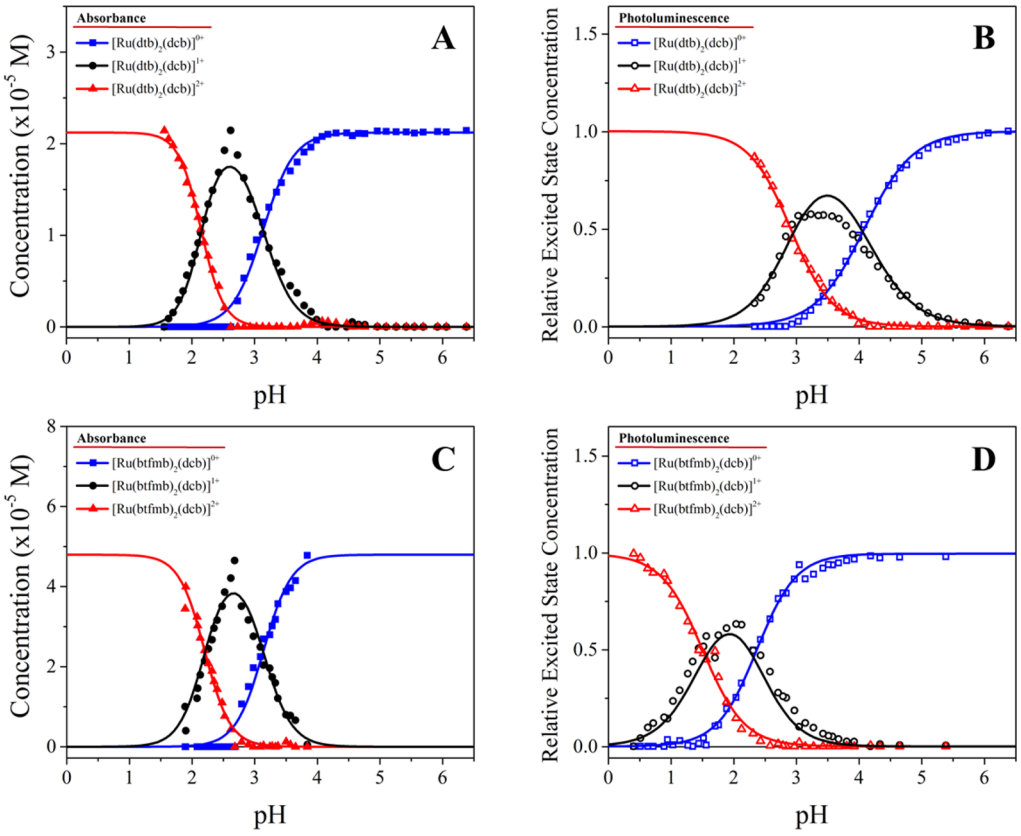

Figure 5. Spectral modeling curves of $[Ru(dtb)_2(dcb)]^{2+}$ (A,B) and $[Ru(btfmb)_2(mcb)]^{2+}$ (C,D) reporting on the ground state concentration (solid symbols) and relative excited state concentration (open symbols) of the indicated protonation states as a function of the pH.

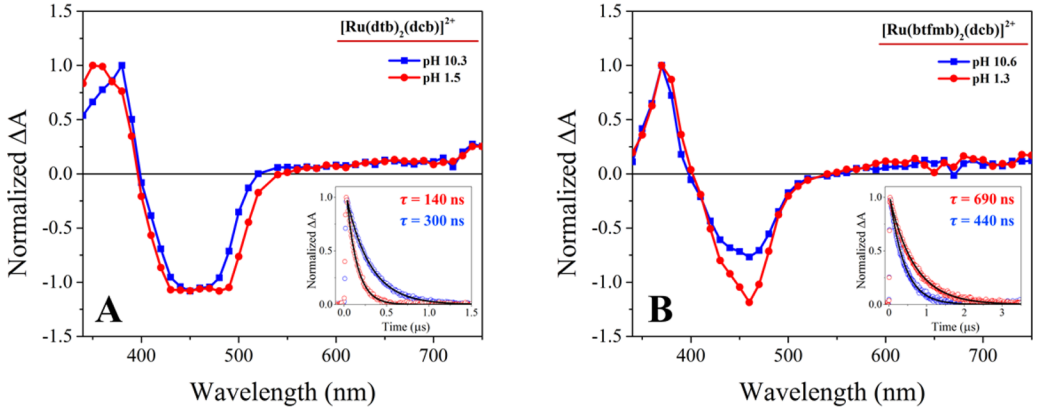

Figure 6. Transient absorption spectra measured 25 ns after pulsed 532 nm light excitation of (A) $[Ru(dtb)_2(dcb)]^{2+}$ and (B) $[Ru(btfmb)_2(dcb)]^{2+}$ under the indicated basic (blue) and acid (red) conditions. The insets display single wavelength kinetics measured at 450 nm at the indicated pH conditions with overlaid fits to a first-order kinetic model.

compounds are given in Figures 4 and 5, respectively. The presence of the monoprotonated compound was clearly identified in the spectral analyses of the dcb compounds.

Figures 4 and 5 also display titration data where the integrated PL intensity was quantified by a full spectral analysis. Care was taken to excite at the ground state isosbestic points so that the excited state concentration remained constant over the entire pH range. The measured PL spectra at any given pH were deconvoluted into the contributions from each emitting species that were then integrated and divided by the known quantum yields. This provided the relative excited state concentrations of each species at each pH. The pH where the concentrations of the excited acid and conjugate base were equal was defined as the pK_a^* value. Given in the Supporting Information is the more common approach of using the PL intensity directly, termed the *raw PLI*. The difficulty with this approach is twofold. First, for these compounds, the PL spectra of all species overlap in energy. This was particularly problematic for the dcb containing compounds where three different species could contribute to the measured intensity at any given wavelength. Second, the PL intensity does not report on concentrations and the inflection points do not yield the pK_a^* values as is described in the Discussion.

Transient absorption difference spectra measured 25 ns after pulsed 532 nm laser excitation of $[Ru^{II}(btfmb)_2(dcb)]^{2+}$ or $[Ru^{II}(dtb)_2(dcb)]^{2+}$ are shown in Figure 6. Clean isosbestic

DOI: 10.1021/jacs.6b00454
J. Am. Chem. Soc. 2016, 138, 3891−3903

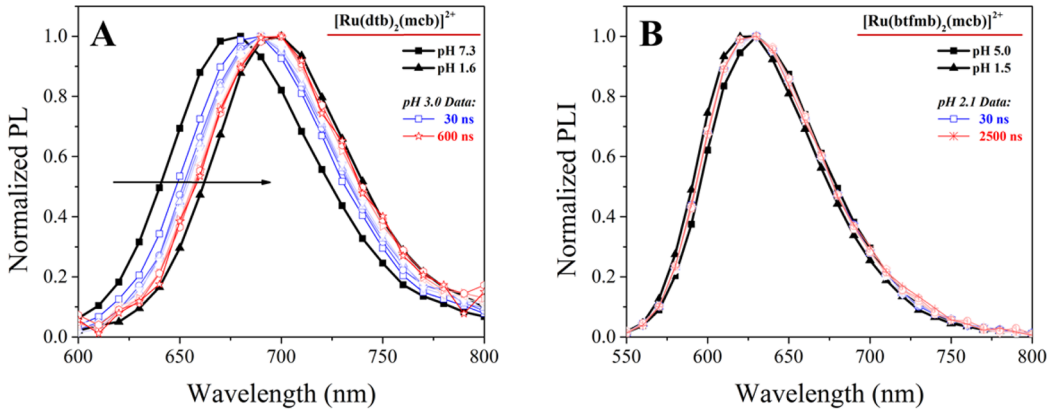

Figure 7. Transient photoluminescence spectra obtained 30 ns (blue squares) and longer (blue to red) time delays after pulsed 532 nm laser excitation of $[Ru(dtb)_2(mcb)]^{2+}$ (A) and $[Ru(btfmb)_2(mcb)]^{2+}$ (B) at the indicated pH value. The time independent spectra of the fully deprotonated and protonated forms obtained after pulsed laser excitation are given for reference under basic (black, square) and acidic (black, up triangle) conditions.

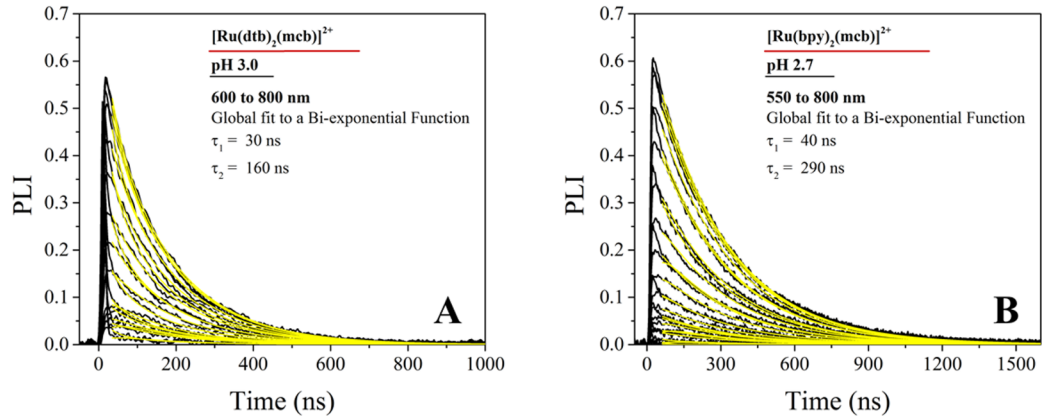

Figure 8. Biexponential global fit of the time-resolved photoluminescence measured as a function of the monitoring wavelength at the indicated pH values with the τ_1 and τ_2 values derived from the coupled system analysis for (A) $[Ru(dtb)_2(mcb)]^{2+*}$ and (B) $[Ru(bpy)_2(mcb)]^{2+*}$.

points were observed around 400 and 530 nm for all compounds studied at pH values less than two or greater than five. The transient absorption spectra were superposable with respect to time, behavior consistent with the formation of a single excited state. The spectra displayed a positive absorption feature below 400 nm that was assigned as a ligand-centered $^3\pi \rightarrow {}^3\pi^*$ transition. Sharp transient absorption features with maxima near 370 nm were observed after pulsed light excitation of both the diprotonated and fully deprotonated forms of $[Ru(btfmb)_2(dcb)]^{2+*}$. In contrast, the normalized spectra of $[Ru(dtb)_2(dcb)]^{2+*}$ revealed an absorption maximum at 380 nm for the diprotonated compound and at 350 nm for the fully deprotonated form. The transient bleach minimum was observed at 450 nm for both forms of $[Ru(dtb)_2(dcb)]^{2+*}$, although the bleach was broader for the protonated form compared to the deprotonated form, consistent with the ground state absorption spectra. Control experiments with $[Ru(bpy)]_3^{2+}$ revealed a pH independent absorption band at 370 nm and a bleach at 450 nm. The first-order excited state relaxation kinetics were observation wavelength independent with abstracted rate constants in excellent agreement with those measured independently by time-resolved photoluminescence.

Photoluminescence spectra of $[Ru(dtb)_2(mcb)]^{2+*}$ measured 25 ns after pulsed laser excitation, are shown in Figure 7A. The normalized photoluminescence spectra at pH 1.6 and 7.3 were superposable with time. The spectra obtained at pH of 3.0 were not superposable and exhibited a significant red-shift with increased time. Note that the PL maxima were not the same as that seen in Table 2 and Figure 2, as they were measured transiently on an apparatus that had not been spectrally corrected. Similar time dependent red shifts in the PL spectra were measured for $[Ru(dtb)_2(dcb)]^{2+*}$, $[Ru(bpy)_2(dcb)]^{2+*}$, and $[Ru(bpy)_2(mcb)]^{2+*}$ at intermediate pH values where excited state acid–base equilibria was expected. In contrast, the PL spectra of the compounds that contained the btfmb ligand were time independent at all pH values measured, even with streak-camera detection that afforded 300 ps time resolution. Representative data for $[Ru(btfmb)_2(dcb)]^{2+*}$ is given in Figure 7B.

Excited state relaxation was found to be nonexponential for the photobasic compounds at pH values where an excited state acid–base equilibrium was expected. Instead, the data was well described by a sum of two first-order rate constants. Shown in Figure 8 are representative PL decays monitored from 600 to 800 nm with overlaid fits to a biexponential kinetic model. This analysis revealed two lifetimes of 40 and 290 ns for $[Ru(bpy)_2(mcb)]^{2+}$ and 30 and 160 ns for $[Ru(dtb)_2(mcb)]^{2+}$, that were independent of the monitoring wavelength.

DISCUSSION

Thorough spectroscopic measurements and kinetic analysis revealed that four of the six ruthenium polypyridyl compounds investigated were less acidic in the excited state, i.e. photobases, while the remaining two were more acidic, that is, photoacids.

DOI: 10.1021/jacs.6b00454
J. Am. Chem. Soc. 2016, 138, 3891–3903

This is unprecedented behavior as decades of research has taught that the identity of the ionizable group regulates excited-state acid−base behavior: all previous organic dyes with conjugated carboxylate groups were identified to be photobases.[66−69] Yet among these closely related compounds this clearly was not the case. The excited state studies reported provide insights into the origins of this new behavior and suggest means by which it can be further optimized for practical and fundamental applications. Also reported is the first quantification of excited state proton transfer in transition metal compounds that provide the kinetic rate constants that control excited state acid−base chemistry and pK_a* values. The photophysical behavior of the compounds is described below followed by the thermodynamics and kinetics.

Photophysical Properties. The photophysical properties reported are characteristic of compounds with low-lying metal-to-ligand charge-transfer (MLCT) excited states that are formally characterized as an oxidized metal center and an electron localized on a single diimine ligand.[70−74] For heteroleptic tris-chelate compounds, the excited state localizes on the most easily reduced ligand on time scales relevant to these studies.[75−81] Nanosecond transient absorption data were consistent with this assertion and the formation of thermally equilibrated MLCT states as shown in eqs 4−6.

$$[Ru^{II}(bpy)_2(dcb)]^{2+} + h\nu \rightarrow [Ru^{III}(bpy)_2(dcb^{-})]^{2+*} \quad (4)$$

$$[Ru^{II}(dtb)_2(dcb)]^{2+} + h\nu \rightarrow [Ru^{III}(dtb)_2(dcb^{-})]^{2+*} \quad (5)$$

$$[Ru^{II}(btfmb)_2(dcb)]^{2+} + h\nu \rightarrow [Ru^{III}(btfmb^{-})(btfmb)(dcb)]^{2+*} \quad (6)$$

Assignments based solely on electronic spectra are not as definitive as those based on time-resolved resonance Raman measurements that provide a direct fingerprint through the vibrational spectrum of the luminescent excited state.[75−81] Nevertheless, the UV absorption band of the excited states were well resolved and characteristic of the reduced ligand present in the excited state, providing compelling evidence for these assignments.[82] In addition, Hammett parameters predict that the electron-withdrawing influence of the 4,4′-substituents should increase in the order *tert*-butyl ($\sigma = -0.20$) < H ($\sigma = 0$) < COOH ($\sigma = 0.45$) < CF_3 ($\sigma = 0.54$),[82] consistent with this interpretation. The ethyl ester group has a Hammett parameter identical to that of the carboxylic acid,[82] so eqs 4−6 also apply to the monocarboxylic acid (mcb) compounds.

The influence of the carboxylate-carboxylic acid equilibrium on the energy gap is of particular interest to this manuscript. For the excited states localized on the dcb or mcb ligand, the more electron withdrawing carboxylic acid stabilizes the excited state relative to the carboxylate consistent with the blue (hypsochromic) shift as the pH was raised. For the excited states localized on the btfmb ligand, radiative decay did not formally involve the dcb or mcb ligand and the observed red (bathochromic) shift with increased pH emanated from a pH induced shift in the ground state $Ru^{III/II}$ potential. The withdrawing nature of the carboxylic acids made oxidation of the metal center more difficult relative to the conjugate carboxylate base. We note that scholarly texts[83] and classical studies[84] have shown that the electron withdrawing nature of a carboxylic acid groups is best understood as a field effect, rather than an inductive effect, that is directly transmitted through space rather than along bonds. In practice, it is difficult to separate these two and herein the term "inductive effect" is utilized to refer to their combined action.

The excited state lifetimes and quantum yields were dictated by the nonradiative rate constants that were about 2 orders of magnitude larger than the radiative rate constants. The k_{nr} values increase exponentially with the energy separation between the ground and excited state in accord with the energy gap law.[63,85−87] Interestingly, at a given energy gap an excited state localized on a dcb (or mcb) ligand had a significantly smaller k_{nr} value than did one localized on a btfmb ligand. For example, a compound that emits red light at 650 nm (~15 400 cm^{-1}) has about twice as long an excited state lifetime when localized on a dcb (or mcb) ligand. This is attributed to a resonance (i.e., mesomeric) effect where conjugation between the carboxylic acid and the pyridine ring result in greater delocalization of the excited state and a longer lifetime.[83] The distortion angle between carboxylic acid groups and the pyridine ring was <10° in solid state $[Ru(bpy)_2(mcb)]^{2+}$, where intermolecular $\pi-\pi$ interactions appear to dominate crystal packing. The excited state structure in aqueous solution is expected to differ. There is in fact compelling evidence for MLCT excited state delocalization onto aromatic substituents in these same 4- and 4′-positions of bipyridine in a manner similar to that envisioned here.[63,88,89]

Thermodynamics. Single inflection and isosbestic points were observed in the spectrophotometric titration data even though two were expected for the compounds with a dcb ligand. Such behavior has previously been reported for the parent compound $[Ru^{II}(bpy)_2(dcb)]^{2+}$,[1,27,34,90] leading to a considerable uncertainty in the true pK_a values. To better understand this chemistry, the mcb ligand that contains one ethyl ester and one carboxylic acid group in the 4- and 4′-positions of bipyridine was synthesized. Indeed the visible absorption spectra of the deprotonated form of compounds with the mcb ligand enabled the monoprotonated dcb compounds absorption spectra to be identified. This spectrum, when combined with the spectra of the diprotonated and fully deprotonated compounds, enabled full spectral simulation of all the titration data that in turn provided accurate determinations of the pK_a values. It is of interest to briefly contrast the values for $[Ru^{II}(bpy)_2(dcb)]^{2+}$ with those previously reported in the literature, Table 5.

Table 5. Ground and Excited State pK_a Values for $[Ru(bpy)_2(dcb)]^{2+}$

compd	pK_{a1}	pK_{a2}	pK_{a1}*	pK_{a2}*	ref
$[Ru(bpy)_2(dcb)]^{2+}$	5.50	5.50	8.50	8.50	27
$[Ru(bpy)_2(dcb)]^{2+}$	1.75	2.80			48
$[Ru(bpy)_2(dcb)]^{2+}$	1.85	2.90	3.60	4.50	32
$[Ru(bpy)_2(dcb)]^{2+}$	1.75	2.85	4.25		31
$[Ru(bpy)_2(dcb)]^{2+}$	0.5	2.65	< 0.2	4.10	33
$[Ru(bpy)_2(dcb)]^{2+}$	2.01	2.83	2.58	3.72	this work

The lack of isosbestic points in the acid base titration of $[Ru^{II}(bpy)_2(dcb)]^{2+}$ led Giordano et al. to model the equilibria as the simultaneous loss of both protons.[27] This analysis resulted in about a factor of 2 error in the reported pK_a values and the incorrect conclusion that the two carboxylic acids had the same ionization constants. Through careful titration studies, Ferguson et al.,[48] Lay and Sasse,[32] and Nazeeruddin and Kalyanasundaram[31] were able to identify both equilibrium processes; the pK_{a2} values reported were in good agreement, while the pK_{a1} values were ~0.25−0.15 pK_a units lower than that reported here, behavior suspected to result from single wavelength rather than full spectral analysis. Shimidzu et al. observed an isosbestic point in very acidic solutions, the nature of which remains unknown.[33]

DOI: 10.1021/jacs.6b00454
J. Am. Chem. Soc. 2016, 138, 3891−3903

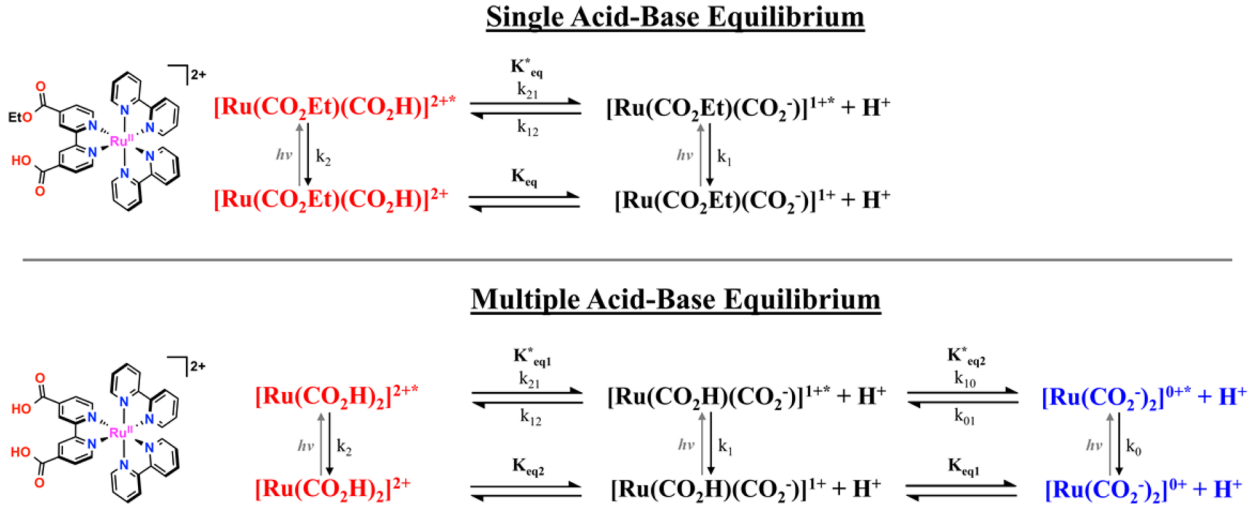

Figure 9. Square scheme for ground and excited state acid–base chemistry of a compound containing one carboxylic acid group (single acid base equilibrium) and two carboxylic acids (multiple acid–base equilibrium).

Photoluminescence (PL) intensity titrations of the dcb containing compounds displayed only a single inflection point when two were expected. Again the mcb compounds were utilized to determine the PL spectra and quantum yields of the monoprotonated dcb-containing compounds that when combined with the other reference spectra enabled the relative excited state concentrations of all the relevant species to be quantified at each pH. A simple PL titration experiment, with light excitation at an isosbestic point, then enabled the direct determination of the pK_a* values by identification of the pH where equal concentrations of the excited carboxylic acid and conjugate base were present. To our knowledge, this approach has not been previously proposed and avoids the uncertainties inherent in alternative pK_a* determinations.

Comparisons of the pK_a* values of $[Ru^{II}(bpy)_2(dcb)]^{2+*}$ with literature reports is revealing in this regard. Previous workers used the pH at the inflection point (pH_i) to determine pK_a* and were cognizant of the fact that the PL intensity did not report directly on concentration. This was accounted for with eq 7, where τ_{HB} and τ_B are the lifetimes of the excited acid and conjugate base.[1,22,91−95]

$$pK_a^* = pH_i + \log\left(\frac{\tau_{HB}}{\tau_B}\right) \quad (7)$$

Derivation of this relation rests on the assumption that an acid–base equilibrium is established in the excited state.[1,22] However, the kinetic data reported here, and discussed in the following section, reveal that an excited state equilibrium for the photobasic compounds is not achieved until after more than one lifetime. As all previously published data utilized eq 7, the usefulness of these reported values is now realized to be in question. We note that excited state equilibria were established for the photoacids in this study, as described below, validating the use of eq 7 for the btfmb compounds reported here for the first time.

An alternative approach for calculation of pK_a* values is the Förster method that uses a thermodynamic cycle with the ground state pK_a and the energy stored in the excited states, eq 8,[1,22,91,94]

$$pK_a^* = pK_a + \left(\frac{1}{2.303RT}\right)(\upsilon_B - \upsilon_{HB}) \quad (8)$$

where R is the gas constant, T is temperature, and ν_B and ν_{HB} correspond to the E_{00} energy of the deprotonated and protonated compounds, respectively. The large spin–orbit coupling induced by the Ru center makes spin a poor quantum number and hence considerable uncertainty in the determination of the *"true"* E_{00} values.[72] A Franck–Condon line shape analysis[62,63] of the corrected PL spectra provided estimates of ν_B and ν_{HB} that were utilized in this calculation, thus qualitatively predicting the photoacid and photobase behavior, with quantitative values for the mcb containing compounds that were only 0.15 pK_a units different from those determined from spectral modeling of the PL titration data.

The pH induced spectral changes are understood based on the nature of the emitting state and the inductive influence of the ionizable groups as was discussed above. Recall that the bathochromic shift of the photoacids results from the inductive influence of acid–base chemistry on the $Ru^{III/II}$ reduction potential. Consistent with this model was the fact that the presence of two carboxylic acid groups in $[Ru^{II}(btfmb)_2(dcb)]^{2+}$ resulted in about twice the ΔpK_a values as that measured for the mcb analogue. Compounds with additional carboxylic acid groups, such as $[Ru^{II}(btfmb)(dcb)_2]^{2+}$ would be expected to give even larger blue shifts in the PL spectra after excited state proton transfer. Similar behavior might have been expected for 4,4′-$(Cl)_2$-2,2′-bipyridine compounds that also possess low-lying π^* orbitals, however no significant spectral shifts were observed and protonation led to an unexpected decrease in PL intensity suggesting some alternative photochemistry.[40] The bathochromic shift expected for photobases was observed for the dtb and bpy compounds reported here and for a much larger number of previously reported dcb containing transition metal compounds.[1,2,27,29−34,40,48,96]

Kinetics. When excited states localized on the dcb or mcb ligands were photogenerated at pH values where acid–base equilibria was relevant, time dependent PL spectral shifts were observed indicating that acid–base chemistry was occurring on the nanosecond time scale. In contrast, no spectral shifts were observed for the btfmb containing compounds, consistent with a more rapid establishment of the excited state equilibrium. These observations provide rough estimates of the rate constants for excited state proton transfer. More precise values have previously been abstracted from PL decays monitored at single observation

DOI: 10.1021/jacs.6b00454
J. Am. Chem. Soc. 2016, 138, 3891−3903

Table 6. Kinetic Parameters Abstracted from the Coupled Systems Model of the Experimental Data

compd	pH[a]	k_1 (s^{-1})	k_2 (s^{-1})	k_{12} (M^{-1} s^{-1})	k_{21} (s^{-1})	K_{eq}	pK_a*
$[Ru(bpy)_2(mcb)]^{2+}$	2.7	2.94×10^6	3.71×10^6	7.83×10^9	7.01×10^6	1.05×10^3	3.03
$[Ru(dtb)_2(mcb)]^{2+}$	3.0	4.72×10^6	6.54×10^6	1.96×10^{10}	5.96×10^6	3.15×10^3	3.49

[a]The pH at which the time-resolved photoluminescence decays were acquired.

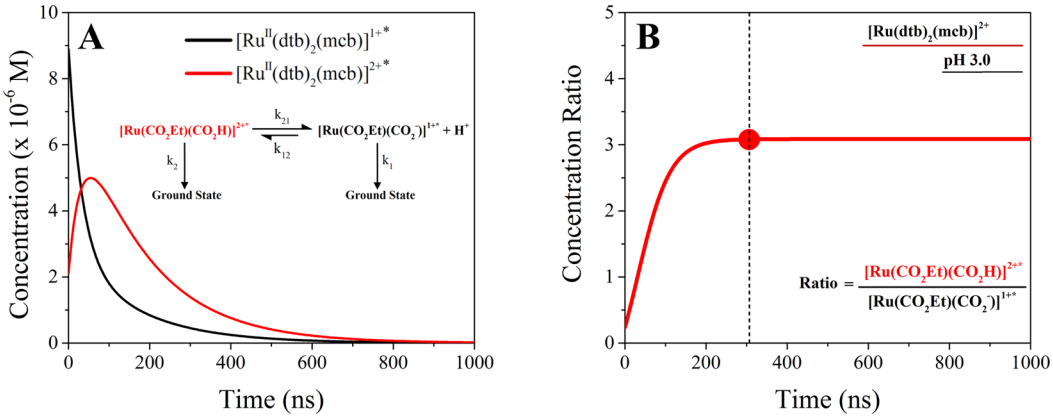

Figure 10. (A) Excited state concentrations of the deprotonated $[Ru(dtb)_2(mcb)]^{+}$*, black, and protonated $[Ru(dtb)_2(mcb)]^{2+}$*, red, compounds abstracted from kinetic analysis of the bi-exponential PL decays measured after pulsed light excitation of $[Ru(dtb)_2(mcb)]^{2+}$. (B) The given excited state concentration ratio as a function of time; the dotted line near 300 ns indicates the time when a steady state quasi-equilibrium was achieved.

wavelengths from organic singlet states.[14,97] Here we apply this analysis to inorganic compounds for the first time and restrict such analysis to the photobasic mcb compounds that were not complicated by a second excited state equilibrium, Figure 9.

The square scheme shown in Figure 9 has been widely used to understand the acid−base chemistry of organic excited states,[14,22,25,97] and is also relevant to other excited state equilibrium processes such as excimer formation. The rate equations that describe the single acid−base equilibrium are given in eqs 9 and 10.

$$\frac{d[A^*]}{dt} = -(k_2 + k_{21})[A^*] + k_{12}[B^*] \quad (9)$$

$$\frac{d[B^*]}{dt} = +k_{21}[A^*] - (k_1 + k_{12})[B^*] \quad (10)$$

For simplification, $[A^*]$ and $[B^*]$ refer to the concentrations of the excited protonated acid, $[Ru(CO_2Et)(CO_2H)]^{2+}$*, and the conjugated base, $[Ru(CO_2Et)(CO_2^-)]^{1+}$*, respectively. The differential equations were solved for the general case where the initial boundary condition accounts for the excitation of both $[A^*](t = 0\ s) = A_0$ and $[B^*](t = 0\ s) = B_0$. For detailed description of the solutions to these coupled differential equations the authors recommend the work of Brand,[14,97] or the text by Demas,[25] that requires knowledge of the excited state concentrations $[A^*]$ and $[B^*]$. Because PL intensities do not report on concentrations, it was necessary to introduce the constants a and b for appropriate conversion. As the measured PL spectra of the acid and conjugate bases overlap in the amplitude at each observation wavelength, $a(\lambda)$ and $b(\lambda)$ were analyzed, eq 11.

$$PLI(\lambda, t) = a(\lambda)\,[A^*](t) + b(\lambda)\,[B^*](t) \quad (11)$$

At pH values were the excited state equilibrium was operative, biexponential kinetics were observed for the photobasic compounds under study consistent with eqs 9 and 10. Biexponential relaxation behavior for Ru polypyridyl excited states were reported in the past,[31,39] although their importance remained unclear. The kinetic data reported here could not be modeled by a weighted sum of the protonated and deprotonated lifetimes of the compound as might naively have been expected. Instead, the two lifetimes abstracted from a biexponential analysis represent the dynamics of the entire system as was first shown in 1972.[14,25,97] The lifetimes τ_1 and τ_2 abstracted from biexponential fits are functions of all the rate constants, k_1, k_2, k_{12}, and k_{21} present in the equilibrium system.[14,22,25,97] Fortunately, the relevant differential equations have previously been solved and allow for a complete system analysis.[14,25,97]

The unimolecular rate constants for deprotonation of $[Ru(dtb)_2(mcb)]^{2+}$* and $[Ru(bpy)_2(mcb)]^{2+}$* of $k_{21} = (5-7) \times 10^6\ s^{-1}$ were at least an order of magnitude smaller than those previously reported for excited phenols and carboxylic acid compounds.[69] The time required to establish steady state concentrations, that is, "quasi-equilibrium", was calculated with the abstracted rate constants in Table 6. Representative data of the time dependent concentrations present after pulsed laser excitation of $[Ru(dtb)_2(mcb)]^{2+}$ are shown in Figure 10. About 300 ns were required for establishment of the quasi-equilibrium and a similar time scale was observed for $[Ru(bpy)_2(mcb)]^{2+}$*. In contrast, the excited-state acid−base equilibrium was established on a sub-300 ps time scale for the btfmb compounds. A plausible explanation for the very disparate time scales for excited state equilibration is that the orientation of the excited-state dipole relative to the ligand that undergoes acid−base chemistry directly influences proton transfer dynamics. When the excited-state dipole was oriented toward the mcb ligand, Coulombic interactions with the proton slowed transfer relative to the situation where the dipole was oriented away from the ionizable ligand. This kinetic data provided pK_a* values that were within 0.1 pK_a units of those abstracted from steady state PL titrations. Indeed self-consistent pK_a* values obtained from PL titrations, Förster cycles, and this kinetic analysis.

The orientation of the excited state dipole relative to the dcb ligand is also relevant to their use in dye-sensitized solar cells

DOI: 10.1021/jacs.6b00454
J. Am. Chem. Soc. 2016, 138, 3891−3903

(DSSCs),[50−52] where it is generally believed that excited state injection is optimal when the charge transfer dipole is oriented toward the semiconductor surface.[98] Since the 2010 report of a 2.4% efficient aqueous DSSC,[99] there has been renewed interest in water-based electrolytes for DSSCs and a review article on this subject has recently appeared.[100] The ground state acid−base chemistry reported here can impact the surface stability of dye molecules, protons are expected to compete with TiO_2 surface states that comprise the carboxylate linkages under pH conditions near and below the ground state pK_a values. Due to the Nernstian shift of the band edge positions with pH, acidic conditions favor excited state injection.[51] In addition, quartz crystal microbalance studies have shown that electron injection into TiO_2 is accompanied by charge-compensating uptake of a proton.[101] It is interesting to consider whether an excited dye molecule that transfers *both* an electron and a proton to the semiconductor surface would be advantageous for DSSCs since such charge neutral reactions are expected to have small reorganization energies. With regard to this study, the $[Ru(dtb)_2(dcb)]^{2+}$ or $[Ru(bpy)_2(dcb)]^{2+}$ have optimal dipole alignment for excited state injection, but their photobasic character would be undesirable for proton transfer to the semiconductor. In contrast, the photoacidic behavior of $[Ru(btfmb)_2(dcb)]^{2+*}$ is ideal for proton transfer, but with a nonoptimal dipole orientation for interfacial electron transfer. New transition metal compounds that vectorially transfer both protons and electrons are hence of interest for applications in DSSCs and other artificial photosynthetic devices.[10,17−19,102]

CONCLUSIONS

Ruthenium polypyridyl compounds were made photobasic or photoacidic through control of the orientation of the charge transfer excited state relative to the ligand with conjugated carboxylic acid groups. Excited states localized on the ligand with the carboxylic acid group were photobases while those localized on an alternative ligand were photoacids. This previously unrecognized behavior provides new opportunities for fundamental and practical applications of these and related transition metal compounds. Studies of how specific buffers influence the excited state proton transfer reactions would be particularly useful for elucidating their role in light driven water splitting and solar fuels production. The pH range and magnitude of ΔpK_a could be further tuned by the incorporation of alternative functional groups, such as amines or phenols. The finding that the excited state need not be localized on the ligand undergoing acid base chemistry implies that a single transition metal compound with three (or more) different acid−base groups could be synthesized and would be responsive at multiple pH values in a predictable fashion.

ASSOCIATED CONTENT

Supporting Information

The Supporting Information is available free of charge on the ACS Publications website at DOI: 10.1021/jacs.6b00454.

Absorption and PL spectra of the de-, mono-, and diprotonated forms of the compounds; plot of the nonradiative rate constant versus the ground-excited state energy gap; absorption and PL titrations; tabulated values of the Franck−Condon line shape analysis of the corrected PL spectra; and tabulated pK_a* values (PDF)
Crystallographic data (CIF)

AUTHOR INFORMATION

Corresponding Author

*gjmeyer@email.unc.edu

Notes

The authors declare no competing financial interest.

ACKNOWLEDGMENTS

The research was part of the UNC EFRC: Center for Solar Fuels, an Energy Frontier Research Center funded by the U.S. Department of Energy (DOE), Office of Science, Basic Energy Sciences BES, under Award DE-SC0001011. R.M.O. would also like to thank the National Science Foundation for an individual Graduate Research Fellowship under Grant No. DGE-1232825. We thank John Papanikolas for use of a streak-camera and Ludwig Brand for stimulating discussions.

REFERENCES

(1) Vos, J. G. *Polyhedron* **1992**, *11*, 2285.
(2) Hicks, C.; Ye, G.; Levi, C.; Gonzales, M.; Rutenburg, I.; Fan, J.; Helmy, R.; Kassis, A.; Gafney, H. D. *Coord. Chem. Rev.* **2001**, *211*, 207.
(3) Greiner, G.; Maier, I. *J. Chem. Soc., Perkin Trans. 2* **2002**, 1005.
(4) Whitaker, J. E.; Haugland, R. P.; Prendergast, F. G. *Anal. Biochem.* **1991**, *194*, 330.
(5) Lakowicz, J. R. In *Principles of Fluorescence Spectroscopy*; Lakowicz, J. R., Ed.; Springer: New York, 2006; p 623.
(6) Crivello, J. V.; Dietliker, K.; Bradley, G. *Photoinitiators for Free Radical Cationic & Anionic Photopolymerisation*; Wiley: New York, 1999; Vol. 3.
(7) Zhou, W.; Kuebler, S. M.; Braun, K. L.; Yu, T.; Cammack, J. K.; Ober, C. K.; Perry, J. W.; Marder, S. R. *Science* **2002**, *296*, 1106.
(8) Nakashima, T.; Tsuchie, K.; Kanazawa, R.; Li, R.; Iijima, S.; Galangau, O.; Nakagawa, H.; Mutoh, K.; Kobayashi, Y.; Abe, J.; Kawai, T. *J. Am. Chem. Soc.* **2015**, *137*, 7023.
(9) Serafinowski, P. J.; Garland, P. B. *J. Am. Chem. Soc.* **2003**, *125*, 962.
(10) Dempsey, J. L.; Winkler, J. R.; Gray, H. B. *J. Am. Chem. Soc.* **2010**, *132*, 16774.
(11) Murtaza, Z.; Chang, Q.; Rao, G.; Lin, H.; Lakowicz, J. R. *Anal. Biochem.* **1997**, *247*, 216.
(12) Bowie, L. J.; Irwin, R.; Loken, M.; DeLuca, M.; Brand, L. *Biochemistry* **1973**, *12*, 1852.
(13) Laws, W. R.; Posner, G. H.; Brand, L. *Arch. Biochem. Biophys.* **1979**, *193*, 88.
(14) Loken, M. R.; Hayes, J. W.; Gohlke, J. R.; Brand, L. *Biochemistry* **1972**, *11*, 4779.
(15) Abeyrathna, N.; Liao, Y. *J. Am. Chem. Soc.* **2015**, *137*, 11282.
(16) Tatum, L. A.; Foy, J. T.; Aprahamian, I. *J. Am. Chem. Soc.* **2014**, *136*, 17438.
(17) Zhou, D.; Khatmullin, R.; Walpita, J.; Miller, N. A.; Luk, H. L.; Vyas, S.; Hadad, C. M.; Glusac, K. D. *J. Am. Chem. Soc.* **2012**, *134*, 11301.
(18) Eisenhart, T. T.; Dempsey, J. L. *J. Am. Chem. Soc.* **2014**, *136*, 12221.
(19) Tolbert, L. M.; Haubrich, J. E. *J. Am. Chem. Soc.* **1994**, *116*, 10593.
(20) Huynh, M. H. V.; Meyer, T. J. *Chem. Rev.* **2007**, *107*, 5004.
(21) Wenger, O. S. *Acc. Chem. Res.* **2013**, *46*, 1517.
(22) Ireland, J. F.; Wyatt, P. A. H. In *Advances in Physical Organic Chemistry*; Gold, V., Ed.; Academic Press: New York, 1976; Vol. *12*, p 131.
(23) Shizuka, H. *Acc. Chem. Res.* **1985**, *18*, 141.
(24) Tolbert, L. M.; Solntsev, K. M. *Acc. Chem. Res.* **2002**, *35*, 19.
(25) Demas, J. N. In *Excited State Lifetime Measurements*; Demas, J. N., Ed.; Academic Press: New York, 1983; p 43.
(26) Peterson, S. H.; Demas, J. N. *J. Am. Chem. Soc.* **1976**, *98*, 7880.
(27) Giordano, P. J.; Bock, C. R.; Wrighton, M. S.; Interrante, L. V.; Williams, R. F. X. *J. Am. Chem. Soc.* **1977**, *99*, 3187.
(28) Giordano, P. J.; Bock, C. R.; Wrighton, M. S. *J. Am. Chem. Soc.* **1978**, *100*, 6960.

DOI: 10.1021/jacs.6b00454
J. Am. Chem. Soc. 2016, 138, 3891−3903

(29) Xie, P.-H.; Hou, Y.-J.; Zhang, B.-W.; Cao, Y. *J. Photochem. Photobiol., A* **1999**, *122*, 169.
(30) Xie, P.-H.; Hou, Y.-J.; Zhang, B.-W.; Cao, Y.; Wu, F.; Tian, W.-J.; Shen, J.-C. *J. Chem. Soc., Dalton Trans.* **1999**, 4217.
(31) Nazeeruddin, M. K.; Kalyanasundaram, K. *Inorg. Chem.* **1989**, *28*, 4251.
(32) Lay, P. A.; Sasse, W. H. F. *Inorg. Chem.* **1984**, *23*, 4123.
(33) Shimidzu, T.; Iyoda, T.; Izaki, K. *J. Phys. Chem.* **1985**, *89*, 642.
(34) Higgins, B.; DeGraff, B. A.; Demas, J. N. *Inorg. Chem.* **2005**, *44*, 6662.
(35) Dixon, E. N.; Snow, M. Z.; Bon, J. L.; Whitehurst, A. M.; DeGraff, B. A.; Trindle, C.; Demas, J. N. *Inorg. Chem.* **2012**, *51*, 3355.
(36) Cargill Thompson, A. M. W.; Smailes, M. C. C.; Jeffery, J. C.; Ward, M. D. *J. Chem. Soc., Dalton Trans.* **1997**, 737.
(37) Kirsch-De Mesmaeker, A.; Jacquet, L.; Nasielski, J. *Inorg. Chem.* **1988**, *27*, 4451.
(38) Peterson, S. H.; Demas, J. N. *J. Am. Chem. Soc.* **1979**, *101*, 6571.
(39) Buchanan, B. E.; Vos, J. G.; Kaneko, M.; van der Putten, W. J. M.; Kelly, J. M.; Hage, R.; de Graaff, R. A. G.; Prins, R.; Haasnoot, J. G.; Reedijk, J. *J. Chem. Soc., Dalton Trans.* **1990**, 2425.
(40) Su, C.-H.; Chen, H.-Y.; Tsai, K. Y.-D.; Chang, I. J. *J. Phys. Chem. B* **2007**, *111*, 6857.
(41) Browne, W. R.; O'Connor, C. M.; Hughes, H. P.; Hage, R.; Walter, O.; Doering, M.; Gallagher, J. F.; Vos, J. G. *J. Chem. Soc., Dalton Trans.* **2002**, 4048.
(42) Cummings, S. D.; Eisenberg, R. *Inorg. Chem.* **1995**, *34*, 3396.
(43) Das, S.; Saha, D.; Mardanya, S.; Baitalik, S. *Dalton transactions* **2012**, *41*, 12296.
(44) Leasure, R. M.; Sacksteder, L.; Nesselrodt, D.; Reitz, G. A.; Demas, J. N.; DeGraff, B. A. *Inorg. Chem.* **1991**, *30*, 3722.
(45) Leavens, B. H.; Trindle, C.; Sabat, M.; Altun, Z.; Demas, J.; DeGraff, B. A. *J. Fluoresc.* **2012**, *22*, 163.
(46) Maity, D.; Bhaumik, C.; Karmakar, S.; Baitalik, S. *Inorg. Chem.* **2013**, *52*, 7933.
(47) Maity, D.; Mardanya, S.; Karmakar, S.; Baitalik, S. *Dalton transactions* **2015**, *44*, 10048.
(48) Ferguson, J.; Mau, A. W. H.; Sasse, W. H. F. *Chem. Phys. Lett.* **1979**, *68*, 21.
(49) Mikšovská, J.; Larsen, R. W. *Inorg. Chem.* **2004**, *43*, 4051.
(50) Grätzel, M. *J. Photochem. Photobiol., C* **2003**, *4*, 145.
(51) Ardo, S.; Meyer, G. J. *Chem. Soc. Rev.* **2009**, *38*, 115.
(52) Hagfeldt, A.; Boschloo, G.; Sun, L.; Kloo, L.; Pettersson, H. *Chem. Rev.* **2010**, *110*, 6595.
(53) Adamson, K.; Dolan, C.; Moran, N.; Forster, R. J.; Keyes, T. E. *Bioconjugate Chem.* **2014**, *25*, 928.
(54) Al-Rawashdeh, N. A. F.; Chatterjee, S.; Krause, J. A.; Connick, W. B. *Inorg. Chem.* **2014**, *53*, 294.
(55) Gillaizeau-Gauthier, I.; Odobel, F.; Alebbi, M.; Argazzi, R.; Costa, E.; Bignozzi, C. A.; Qu, P.; Meyer, G. J. *Inorg. Chem.* **2001**, *40*, 6073.
(56) Swords, W. B.; Li, G.; Meyer, G. J. *Inorg. Chem.* **2015**, *54*, 4512.
(57) Benson, E. E.; Grice, K. A.; Smieja, J. M.; Kubiak, C. P. *Polyhedron* **2013**, *58*, 229.
(58) Furue, M.; Maruyama, K.; Oguni, T.; Naiki, M.; Kamachi, M. *Inorg. Chem.* **1992**, *31*, 3792.
(59) Crosby, G. A.; Demas, J. N. *J. Phys. Chem.* **1971**, *75*, 991.
(60) Ardo, S.; Sun, Y.; Staniszewski, A.; Castellano, F. N.; Meyer, G. J. *J. Am. Chem. Soc.* **2010**, *132*, 6696.
(61) Lee, E. C.; Kim, D.; Jurečka, P.; Tarakeshwar, P.; Hobza, P.; Kim, K. S. *J. Phys. Chem. A* **2007**, *111*, 3446.
(62) Johansson, P. G.; Zhang, Y.; Meyer, G. J.; Galoppini, E. *Inorg. Chem.* **2013**, *52*, 7947.
(63) Damrauer, N. H.; Boussie, T. R.; Devenney, M.; McCusker, J. K. *J. Am. Chem. Soc.* **1997**, *119*, 8253.
(64) Forster, L. S. *Coord. Chem. Rev.* **2006**, *250*, 2023.
(65) Yersin, H.; Gallhuber, E. *J. Am. Chem. Soc.* **1984**, *106*, 6582.
(66) Kovi, P. J.; Schulman, S. G. *Anal. Chem.* **1973**, *45*, 989.
(67) Marzzacco, C. J.; Deckey, G.; Halpern, A. M. *J. Phys. Chem.* **1982**, *86*, 4937.
(68) Watkins, A. R. *J. Chem. Soc., Faraday Trans. 1* **1972**, *68*, 28.
(69) Arnaut, L. G.; Formosinho, S. J. *J. Photochem. Photobiol., A* **1993**, *75*, 1.
(70) Caspar, J. V.; Meyer, T. J. *J. Am. Chem. Soc.* **1983**, *105*, 5583.
(71) Durham, B.; Caspar, J. V.; Nagle, J. K.; Meyer, T. J. *J. Am. Chem. Soc.* **1982**, *104*, 4803.
(72) Hager, G. D.; Crosby, G. A. *J. Am. Chem. Soc.* **1975**, *97*, 7031.
(73) Juris, A.; Balzani, Y.; Barigelletti, F.; Campagna, S.; Belser, P.; Von Zelewsky, A. *Coord. Chem. Rev.* **1988**, *84*, 85.
(74) Van Houten, J.; Watts, R. J. *J. Am. Chem. Soc.* **1976**, *98*, 4853.
(75) Bradley, P. G.; Kress, N.; Hornberger, B. A.; Dallinger, R. F.; Woodruff, W. H. *J. Am. Chem. Soc.* **1981**, *103*, 7441.
(76) Dallinger, R. F.; Woodruff, W. H. *J. Am. Chem. Soc.* **1979**, *101*, 4391.
(77) Schoonover, J. R.; Bignozzi, C. A.; Meyer, T. J. *Coord. Chem. Rev.* **1997**, *165*, 239.
(78) McClanahan, S. F.; Dallinger, R. F.; Holler, F. J.; Kincaid, J. R. *J. Am. Chem. Soc.* **1985**, *107*, 4853.
(79) Danzer, G. D.; Kincaid, J. R. *J. Phys. Chem.* **1990**, *94*, 3976.
(80) Mabrouk, P. A.; Wrighton, M. S. *Inorg. Chem.* **1986**, *25*, 526.
(81) Smothers, W. K.; Wrighton, M. S. *J. Am. Chem. Soc.* **1983**, *105*, 1067.
(82) Hansch, C.; Leo, A.; Taft, R. W. *Chem. Rev.* **1991**, *91*, 165.
(83) Lowry, T. H.; Richardson, K. S. *Mechanism and Theory in Organic Chemistry*, 3rd ed.; Benjamin-Cummings Publishing Company: San Francisco, 1997.
(84) Cole, T. W.; Mayers, C. J.; Stock, L. M. *J. Am. Chem. Soc.* **1974**, *96*, 4555.
(85) Caspar, J. V.; Meyer, T. J. *Inorg. Chem.* **1983**, *22*, 2444.
(86) Kober, E. M.; Caspar, J. V.; Lumpkin, R. S.; Meyer, T. J. *J. Phys. Chem.* **1986**, *90*, 3722.
(87) Bixon, M.; Jortner, J. *J. Chem. Phys.* **1968**, *48*, 715.
(88) Strouse, G. F.; Schoonover, J. R.; Duesing, R.; Boyde, S.; Jones, W. E., Jr.; Meyer, T. J. *Inorg. Chem.* **1995**, *34*, 473.
(89) Treadway, J. A.; Loeb, B.; Lopez, R.; Anderson, P. A.; Keene, F. R.; Meyer, T. J. *Inorg. Chem.* **1996**, *35*, 2242.
(90) Xie, P.-H.; Hou, Y.-J.; Zhang, B.-W.; Cao, Y.; Wu, F.; Tian, W.-J.; Shen, J.-C. *J. Chem. Soc., Dalton Trans.* **1999**, 4217.
(91) Förster, T. *Naturwissenschaften* **1949**, *36*, 186.
(92) Weller, A. *Z. Elektrochem.* **1952**, *56*, 662.
(93) Weller, A. *Z. Elektrochem.* **1954**, *58*, 849.
(94) Förster, T. *Z. Elektrochem.* **1950**, *54*, 42.
(95) Förster, T. *Z. Elektrochem.* **1950**, *54*, 531.
(96) Zheng, G. Y.; Wang, Y.; Rillema, D. P. *Inorg. Chem.* **1996**, *35*, 7118.
(97) Laws, W. R.; Brand, L. *J. Phys. Chem.* **1979**, *83*, 795.
(98) Mathew, S.; Yella, A.; Gao, P.; Humphry-Baker, R.; CurchodBasile, F. E.; Ashari-Astani, N.; Tavernelli, I.; Rothlisberger, U.; NazeeruddinMd, K.; Grätzel, M. *Nat. Chem.* **2014**, *6*, 242.
(99) Law, C.; Pathirana, S. C.; Li, X.; Anderson, A. Y.; Barnes, P. R. F.; Listorti, A.; Ghaddar, T. H.; O'Regan, B. C. *Adv. Mater.* **2010**, *22*, 4505.
(100) Bella, F.; Gerbaldi, C.; Barolo, C.; Gratzel, M. *Chem. Soc. Rev.* **2015**, *44*, 3431.
(101) Lemon, B. I.; Hupp, J. T. *J. Phys. Chem.* **1996**, *100*, 14578.
(102) Valdez, C. N.; Schimpf, A. M.; Gamelin, D. R.; Mayer, J. M. *J. Am. Chem. Soc.* **2016**, *138*, 1377.

DOI: 10.1021/jacs.6b00454
J. Am. Chem. Soc. 2016, 138, 3891−3903